

Article

Multi-Objective Resource Scheduling for IoT Systems Using Reinforcement Learning [†]

Shaswot Shresthamali ^{1,*} , Masaaki Kondo ¹ and Hiroshi Nakamura ²

¹ Department of Information and Computer Science, Faculty of Science and Technology, Keio University, Kanagawa 223-8522, Japan

² Department of Information Physics and Computing, Graduate School of Information Science and Technology, The University of Tokyo, Tokyo 113-8656, Japan

* Correspondence: shaswot@acsl.ics.keio.ac.jp

[†] This paper is an extended version of our paper published in 2021 IEEE 14th International Symposium on Embedded Multicore/Many-Core Systems-on-Chip (MCSoc), Singapore, 20–23 December 2021.

Abstract: IoT embedded systems have multiple objectives that need to be maximized simultaneously. These objectives conflict with each other due to limited resources and tradeoffs that need to be made. This requires multi-objective optimization (MOO) and multiple Pareto-optimal solutions are possible. In such a case, tradeoffs are made w.r.t. a user-defined preference. This work presents a general Multi-objective Reinforcement Learning (MORL) framework for MOO of IoT embedded systems. This framework comprises a general Multi-objective Markov Decision Process (MOMDP) formulation and two novel low-compute MORL algorithms. The algorithms learn policies to tradeoff between multiple objectives using a single preference parameter. We take the energy scheduling problem in general Energy Harvesting Wireless Sensor Nodes (EHWSNs) as a case example in which a sensor node is required to maximize its sensing rate, and transmission performance as well as ensure long-term uninterrupted operation within a very tight energy budget. We simulate single-task and dual-task EHWSN systems to evaluate our framework. The results demonstrate that our MORL algorithms can learn better policies at lower learning costs and successfully tradeoff between multiple objectives at runtime.

Keywords: multi objective optimization; multi-objective reinforcement learning; wireless sensors; energy harvesting



Citation: Shresthamali, S.; Kondo, M.; Nakamura, H. Multi-Objective Resource Scheduling for IoT Systems Using Reinforcement Learning. *J. Low Power Electron. Appl.* **2022**, *12*, 53. <https://doi.org/10.3390/jlpea12040053>

Academic Editors: Lan-Da Van, Khanh N. Dang and Kun-Chih Chen

Received: 30 August 2022

Accepted: 29 September 2022

Published: 8 October 2022

Publisher's Note: MDPI stays neutral with regard to jurisdictional claims in published maps and institutional affiliations.



Copyright: © 2022 by the authors. Licensee MDPI, Basel, Switzerland. This article is an open access article distributed under the terms and conditions of the Creative Commons Attribution (CC BY) license (<https://creativecommons.org/licenses/by/4.0/>).

1. Introduction

The deployment of Internet of Things (IoT) devices has increased dramatically in these recent years for a wide variety of applications. A large fraction of these devices are low-power embedded edge devices. In addition to their primary tasks (such as sensing, control, and edge-processing), these devices also need to coordinate auxiliary tasks such as communication, pre-processing, and energy management [1,2]. These embedded systems need to maximize multiple objectives which conflict with each other for limited resources such as energy, bandwidth, and computation time. For instance, in many cases, energy is usually in short supply and needs to be scheduled among many tasks to satisfy different objectives. Take for example a solar-powered temperature sensor that encodes and compresses the sensed data before transmitting it to a server. The nodes need to decide on whether to spend their limited energy on increasing the sensing rate (for more accurate and precise readings) or the transmission power (to compensate for a noisy channel and meet latency requirements) or its CPU frequency (for faster and more efficient data compression). These are multiple task objectives that need to be optimized simultaneously. However, all these tasks share a common limited energy pool which gives rise to resource conflicts. Thus, the user needs to make tradeoffs w.r.t. a preference or *priority*. This requires Multi-objective Optimization (MOO). Unlike single objective optimization problems, it is

not possible to arrive at a globally optimal solution. Instead, there exists multiple optimal solutions with different tradeoffs and the most appropriate one is chosen depending on the user's preference.

Heuristic MOO solutions (e.g., Evolutionary Algorithms (EA), Particle Swarm Optimization (PSO)) are not very suitable MOOs in embedded devices. This is because optimization problems for embedded systems require dynamic *time-variant* objective functions, i.e., the problem parameters, constraints, user preferences, and the set of optimal solutions change at each timestep. For example, the solar-powered node mentioned earlier may have to switch to a different energy budgeting policy whenever the energy availability varies. In such cases, traditional MOO energy scheduling methods need to recompute their solutions as soon as the problem parameters change. This is not practical because this requires a lot of computation, and the time required to optimize and converge to a solution may be insufficient before the next change.

An alternative MOO method is to use Multi-objective Reinforcement Learning (MORL) [3]. Reinforcement Learning (RL) methods [4] are preferable over heuristics because a node can learn policies for many diverse application scenarios, with minimal human supervision, with a common learning framework. An RL agent (the IoT node in this case) uses trial-and-error to explore various optimization policies through direct interaction with the environment. The agent learns progressively better policies using a reward signal as feedback. Single objective RL (SORL) solutions are relatively straightforward and have been researched extensively for ENO in EHWSNs [5–11]. MOO problems are more complex and naive MORL methods have very high computation requirements [12,13] and limited application scope (e.g., discrete state-action spaces [14]) making them unsuitable for embedded systems. Furthermore, both SORL and MORL methods reliably converge to stable solutions only under very idealized conditions. This usually means (i) the interacting environment is a reliably stationary process; (ii) the feedback can be expressed as an easy-to-define reward in a timely manner and (iii) mistakes made during the training phase (exploration) do not have drastic real-world consequences. Video games and board games are good examples of such ideal environments where RL has been very successful and achieved superhuman performance [15,16].

Unfortunately, embedded IoT systems do not have such ideal conditions for learning. They interact in the real environment which is highly unreliable and unpredictable with many one-off events, and the optimality of a policy can be judged only in the long run so the feedback is very delayed and noisy. Furthermore, the nodes have to learn stable convergent policies quickly while avoiding catastrophic mistakes which have real-world consequences as much as possible (e.g., node shutdowns due to energy depletion). Thus, using RL for IoT systems requires two major considerations:

- The RL Markov Decision Process (MDP) must be carefully defined such that it defines the optimization problem accurately and sufficiently, and
- RL algorithms should be able to learn stable policies within reasonable computational costs using the MDP.

With this in mind, we present a general MORL framework for MOO in IoT embedded systems. For the sake of example, we focus on the energy scheduling problem in Energy Harvesting Wireless Sensor Nodes (EHWSNs). This is because MOO for long-term energy-neutral operation in EHWSNs captures some of the most challenging and interesting aspects of using MORL in IoT embedded systems. EHWSNs are sensor nodes that harvest energy from the environment for long-term sensing applications. EHWSNs have had enormous success in a variety of applications such as animal monitoring, personal health care, disaster prevention, etc. [17]. This is because they have an inexhaustible energy source coupled with wireless connectivity which makes them capable of perpetual autonomous operation. However, the uninterrupted perpetual operation requires judicious management of its limited energy resources. This is referred to as Energy Neutral Operation (ENO) [18]. ENO requires the average consumption of energy to be equal to the average harvested supply. It

should also satisfy causality constraints i.e., total consumed energy is always less than or equal to total harvested energy.

ENO for EHWSNs using MORL is a difficult problem because the nodes have very tight energy budgets due to limited battery size and a highly unpredictable and variable ambient energy source. It is necessary for these nodes to intelligently allocate their energy to multiple tasks while remaining energy-neutral (Figure 1). Furthermore, ENO is difficult to express in terms of a reward signal and it requires very long-term planning for energy optimization. It is not clear how the problem should be defined as an MDP, i.e., how to define the states, actions, and rewards; and what RL algorithms are suitable to learn policies that can easily tradeoff over the space of user preferences.

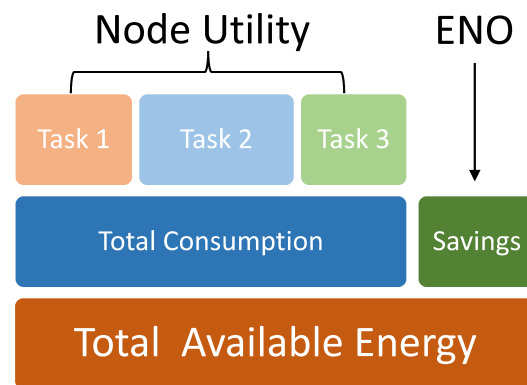


Figure 1. A multi-task EHWSN has to wisely determine its gross energy consumption at each time step so as to remain energy-neutral. Furthermore, it has to proportion the energy among different tasks to maximize node utility.

In this work, we implement our proposed MORL framework for EHWSNs and develop MORL methods to derive solutions that

- ensure that the node does not violate energy neutrality in the long-term by regulating the gross node energy consumption
- proportion of the budgeted energy between different tasks.
- dynamically tradeoff between maximization of different objectives w.r.t. user-defined priorities.
- achieve all of this using much fewer computational requirements than existing methods.

We use a general EHWSN model described in [19], and:

- develop a suitable MDP for both SORL and MORL implementations. Furthermore, we perform comprehensive experiments to analyze how our proposed MDP overcomes the limitations of traditional definitions to achieve near-optimal solutions.
- analyze the effect that different reward incentives and environmental factors have on the learning process as well as the resultant policies.
- demonstrate that our proposed algorithms can overcome the limitation of traditional MORL methods for ENO and learn better policies at lower costs.

We organize this work as follows. In Section 2, we briefly discuss previous research in the area and its limitations. We describe the general EHWSN system model in Section 3 for which we develop our MORL framework. We give a brief theoretical background for ENO and RL in Section 4. In Section 5, we describe the MDP and our proposed algorithms that constitute the MORL framework. The experimental setup is explained in Section 6. We then simulate single-task and dual-task EHWSNs extensively using our proposed framework. We give a comprehensive analysis of our results in Section 7 our conclusions in Section 8.

2. Related Work

2.1. Analytical Methods for ENO

Historically, ENO of EHWSNs maximized a single objective using analytical methods. They focused on maximization of either the gross device energy consumption [18,20] or the communication performance [21,22] using linear programming [18], non-linear programming [23,24], search methods [25], control systems [20], dynamic programming [26,27] among other methods. While these approaches had comprehensive problem statements with formal proofs, they were very application-specific and required significant hand-tuning as well as non-causal information. We base our work on the mathematical foundation and the ENO goals in [18]. The authors provide a linear programming optimization approach that makes use of non-causal environmental data. They estimate the anticipated energy output and choose the duty cycle accordingly. They cater to battery inefficiencies and permit duty cycle adjustments to account for any variations in anticipated and actual harvesting circumstances. However, the efficacy of this method is highly dependent on the prediction mechanism and historical data. A non-causal solution proposed in [20] specified a battery-centric objective function. They restate ENO as a control system problem that minimizes the deviations in the battery level and achieves energy neutrality by using a linear quadratic tracker. The control system is reactive and somewhat adaptive to solar energy fluctuations. However, its stability requires careful calibration of hyperparameters depending upon the working environment. Similar control system solutions are also presented in [28,29]. Our RL-based solution relies very little on the prediction mechanism and any hyperparameter tuning required is a one-time effort. It therefore can be applied across many different application domains with little to no change.

In [29], the authors extend the problem statement by incorporating the *time-varying utility* of the data gathered by the sensor node. They argue that the sensing rate should vary depending on the utility of the sensed data as perceived by the user. They take the example of a soil moisture sensor system that exploits the prior knowledge of the seasonal cycles of rainfall. In this scenario, the utility of sensed data is low when there is no rainfall. Therefore, the authors propose a heuristic solution that conserves energy by reducing the duty cycle when there is little rainfall (low data utility) and increasing the duty cycle when there is rain (high data utility). Although data-utility is an important parameter to consider during energy scheduling, we do not always know how the data utility varies. This work assumes prior knowledge of this variation. Our proposed solution on the other hand does not require any prior information and optimizes the energy policy even if the data utility may vary unexpectedly.

2.2. Single Objective RL Methods for ENO

Analytical methods are unscalable and non-adaptive solutions that require significant design bias. RL methods emerged as an alternative on account of its common algorithmic paradigm to *learn* adaptive policies that could be applied to a wide variety of applications (i.e., scalable solutions). Early applications of RL in EHWSNs concentrated on optimizing simple communication policies [30–35] under the assumption that communication tasks consume the majority of the energy. These methods were superior to analytical methods but required complicated hand-crafted definitions of the states, actions, and reward functions. Since EHWSNs interact with the real world (i.e., an open system), it is very difficult to define the states and actions for an RL MDP that can sufficiently capture the environment dynamics without making the RL problem too complex to solve. More importantly, the ENO reward feedback is very long-term and delayed and so it is difficult to define a reward function for convergent, stable, and robust RL solutions. Non-optimal definitions result in increased learning costs for the nodes which translate to increased learning time, computation requirements, and “catastrophic mistakes” (unsafe exploration actions) made during learning.

Solutions presented in [26,36] use specialized reward functions that are difficult to design. They may also sometimes lead to unexpected behavior due to reward hacking [37–39].

In our previous paper [9], we devised a simpler, general reward function capable of learning adaptive policies using tabular RL. The paper also demonstrated the adaptivity of RL algorithms to changes in climate, device parameters, and battery degradation. Other similar research related to RL for ENO include [40–42].

2.3. Multi-Objective Optimization Methods

Most research related to ENO of EHWSNs (both analytical and RL-based) approaches usually assume maximization of some single proxy objective such as duty cycle/sampling rate [7–9,40,42–44] or communication-based metric such as maximizing throughput/bitrate and minimizing packet loss/latency [5,6,45–49]. However, realistic implementations usually require optimizing over multiple objectives. There has not been enough research on energy scheduling among multiple tasks w.r.t. different objectives in EHWSNs. This is very important, especially for modern resource-constrained sensor nodes.

It is still not very clear what is the best way to learn policies using multiple sources of reward signals. One common approach is to employ *scalarization* techniques to transform the multi-objective problem statement into a single-objective one, and then apply conventional RL algorithms to solve it. Scalarization consolidates the multiple rewards by some function to a single value [7,50–52].

One scalarization technique is to multiply the rewards together and scale the product as in [7,50,52]. In such a case, it is not very clear what objective is being emphasized. These methods do not allow for the optimization of any one specific preference; instead, they learn an “average” policy across the space of preferences. Another scalarization approach is to multiply the rewards by different weights and sum them together [51]. This allows the user to specify which rewards the policy should emphasize i.e., tradeoff between different maximization objectives. However, this requires the relative weights of the different rewards to be known before training. The learning process would have to be repeated separately for different weight configurations. Consequently, the user has to store a different policy for each unique preference which is unscalable and resource intensive. Ideally, we would like an RL method that can trade off between the maximization of different objectives during runtime (after the node has been trained and deployed). Thus reward scalarization methods have significant drawbacks that hinder their use for MORL in EHWSNs. This is explored in more detail in [3,52].

Another method to learn from multiple reward signals would be to integrate them into the RL MDP as a reward *vector*. Such MORL methods are generally available as single-policy methods and multi-policy methods. Interested readers can find a good overview of general MORL methods in [53]. With single policy techniques, the agent learns policies for multiple conflicting objectives whose preferences are not known a priori. However, it is difficult for a single model to learn the best policies for various preference scenarios. These methods generally involve learning an action-value function that takes into account the relative emphasis among the objectives [14,54,55]. For e.g., in [14], the authors modify the Bellman equation to learn a single parametric representation for optimal policies over the space of all possible preferences. They evaluate their method for video game domain problems. A limitation of this work is that the proposed MDP and the corresponding multi-objective Bellman equation are applicable only for *discrete* action spaces where performing an argmax search over the Q-values is feasible. This does not hold for continuous action spaces. We would like a general MORL method that accommodates both continuous states and action spaces. Multi-policy methods learn a *set* of policies in order to approximate the Pareto-frontier [12,13,56–58]. The computed policies encompass the entire space of possible preferences. These methods require considerable computation resources and have scalability issues because the learned policies can grow significantly with the domain size. For example, in [58], the authors propose to decompose a MOO problem into several simpler single-objective problems and solve for each Pareto solution using DRL. They then propose to generate the Pareto-frontier by combining the different Pareto solutions. Since this is a computationally expensive process, they propose to reuse weights of neighboring

sub-solutions to accelerate the convergence of each of the Pareto solutions. Furthermore, they argue that DRL has good generalization properties and can be extended to more complex optimization with no training. This work has a similar approach to MOO as our method in that it interpolates between different Pareto solutions to find a locally optimal one. However, the method in [58] is quite difficult to implement in IoT embedded devices because it employs computationally intensive techniques such as *attention mechanism* and recurrent NN in addition to the actor-critic model. Furthermore, due to the time-varying objective functions in embedded systems, it would be very difficult to compute the solutions from all the sub-models at every timestep. Our method sidesteps this issue by computing only the greediest Pareto solutions and interpolating between them. While this sacrifices some optimality, our method is less compute-intensive.

Contemporary MORL methods are insufficient to solve the ENO problem for MDPs due to a limited MDP and high computation requirements. We, therefore, use our MORL framework to solve the energy scheduling issue for EHWSNs in this work. Our system uses a standard Deep Deterministic Policy Gradient (DDPG) algorithm [59]. DDPG has been used for single reward maximization in [46,47] for communication tasks. Here, we use DDPG for MORL primarily because it can accommodate continuous states and actions while being comparatively less computationally intensive. More powerful RL algorithms are also available, but they require significantly more computational resources.

In [60], the authors also use DDPG to learn multiple tasks from reward vectors. Similar to our approach, they also use a reward vector to learn multiple value functions simultaneously. This is in contrast to standard single-objective RL methods that use a *scalar* reward signal to learn a single value function. However, this work focuses on *multi-task* learning. It assumes the tasks are exclusive (i.e., do not occur simultaneously) and independent (i.e., the objectives are non-conflicting and therefore no tradeoffs are necessary). In short, this work is not a multi-objective optimization problem where tradeoffs need to be made.

Our work is also closely related to [61]. They also use MORL DDPG for an autonomous driving application scenario. In this work, different agents learn policies for different tasks and collectively form a combined policy. However, their method uses a Thresholded Lexicographic Ordering (TLO) method. This requires the user to specify the preferred ordering over objectives and their thresholds prior to training. As explained previously, this is generally not possible because the users usually adjust their preference *after* the node has been deployed. The alternative of storing policies for all possible orders and thresholds is not scalable.

Our proposed MORL MDP and algorithms can learn intelligent policies at lower costs by using continuous state and action spaces from multiple reward sources using a reward vector. Furthermore, our proposed algorithms can learn to tradeoff between multiple objectives at runtime, similar to single-policy MORL methods but using much less computational resources than single-policy and multi-policy methods.

Since we concentrate on MOO with MORL in this work, we have yet to address issues of intermittent computing, task dependency, and network-based optimizations in IoT systems. An alternative approach for consolidating multiple objectives may be a game-theoretic/multi-agent approach as explored in [62,63].

Although we have focused our discussion on MOO for energy scheduling in EHWSNs until now, MOO solutions are quite popular in IoT systems when they focus on holistic network performance rather than individual node energy-neutrality. These works primarily target issues like sensor node deployment configuration to maximize coverage and lifetime [64–66] or optimizing the routing parameters while reducing the latency and energy consumption [67,68]. It is possible to solve these problems with traditional heuristics because they are defined with time-invariant objective functions [69,70]. As to our knowledge, MOO in IoT systems for optimization problems with time-variant objective functions (e.g., duty cycling optimization for EHWSNs) has not been discussed enough. Hence,

we propose our low compute MORL framework to optimize problems with time-varying objective functions.

3. System Model

Figure 2 assumes a harvest-store-use solar EHWSN that is required to be always on. Although this system model is specific to multi-task EHWSNs for optimizing energy usage, it can be easily adapted for other resource-scheduling problems in IoT embedded systems. The EHWSN is equipped with an energy harvester and a finite energy buffer. We assume a battery for the sake of example but any other type of energy buffer can also be used (e.g., super-capacitors). The user requests the node to execute various tasks relating to sensing, communication, and processing. Each task request has an associated energy *demand* to satisfy various performance requirements (e.g., sensing rates [29] and transmission throughputs [6,7]).

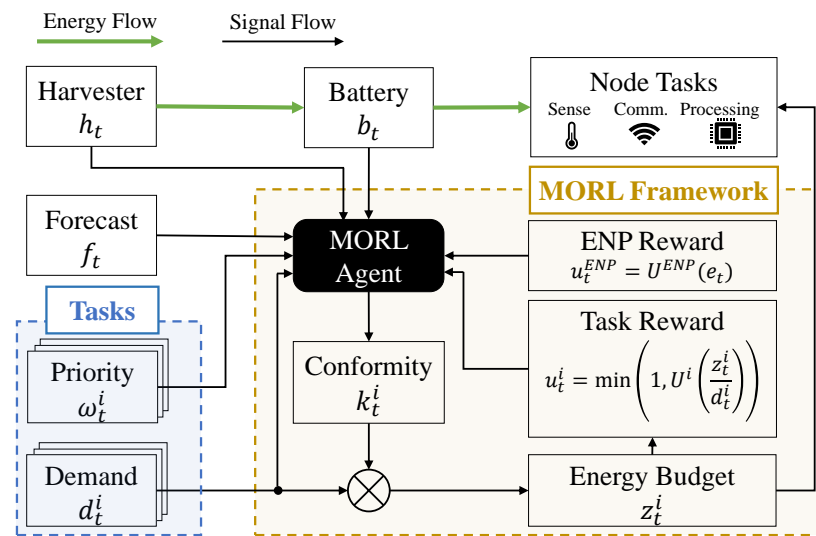


Figure 2. A general system model for multi-task EHWSNs.

The MORL agent optimizes energy usage in discrete timesteps. It intelligently distributes the energy across various tasks at each timestep. Each task generates a *task-utility* depending on how much energy it was allocated. The weighted sum of all task-utilities gives the *node-utility*. The agent's objective is to maximize node utility.

The energy required to fully conform to the user's request to execute the i th task is $d_t^i \in [z_{min}^i, z_{max}^i]$. d_t^i is determined by the user/application and generally varies with time [7,29]. For example, a sensing task request may have a high energy demand d corresponding to an increased sensing duty cycle; or the user may request a higher QoS thus increasing the energy demand for a transmission task.

The MORL agent observes its environment (the system state) at timestep t to decide the task energy, $z_t^i \in [z_{min}^i, z_{max}^i]$. It can under-provision a task to conserve energy by sacrificing task performance. The amount of under-provisioning is represented by the conformity factor $k_t^i \in [0, 1]$. The actual energy allocated to task i is $z_t^i = \max(z_{min}^i, d_t^i \times k_t^i)$. z_{min}^i represents the minimum energy required to run the task. (If $z_t^i < z_{min}^i$, the task fails.) The task-utility is given by $u_t^i = \min(1, U^i(z_t^i/d_t^i))$, where U^i is a monotonically non-decreasing function. Since over-provisioning energy to a task does not result in increased utility, we constrain the task-utility to be $u_t^i \leq 1$.

Our proposed system model improves over traditional system models by explicitly allowing the agent to under-provision the task energy and also preventing any over-provisioning. Traditional solutions usually did not consider the time-varying utilities of tasks and opportunistically maximized duty cycles [8,9]. For e.g., if the objective were to maximize the sensing rate, the node would reactively increase the sensing rate whenever

energy is available [9,18,20] without taking into account whether the sensed data was useful to the user or not. However, as pointed out in [7,29], task utilities generally vary with time and it would be wiser to expend energy in periods of high utility over low utility. With our system model, it is possible for the MORL agent to under-provision tasks that have lower priority/utility for energy savings.

Energy Neutral Operation

For a node with n tasks, at time t , the battery level is $b_t \in [0, b_{max}]$, the harvested energy is $h_t \in [0, h_{max}]$, the total energy demand is $d_t = \sum_{i=1}^n d_t^i$ and the energy consumed by the node is $z_t = \sum_{i=1}^n z_t^i$ s.t. $z_{min} \leq z_t \leq z_{max}$. The charging/discharging losses of the battery are characterized by a function $\mathcal{B}()$. The energy dynamics of the system are therefore given by $b_{t+1} = \min(b_t + \mathcal{B}(h_t - z_t), b_{max})$.

Perfect energy-neutrality is guaranteed if $h_t - z_t = 0 \forall t$ although this might not always be possible or even desirable. For instance, the node must generally maintain a minimum level of operation at all times i.e., $z_{min} > 0$ to account for the energy spent during sleep/listening mode or by the base sensing rate [10]; or the node may need to operate during the night ($h_t < z_t$). In other situations, it might not be best to greedily consume all the energy that has been harvested because some of it might be stored and used to extract more utility in the future. However, the node is energy-neutral if $\mathbb{E}[z] = \mathbb{E}[h]$ where $\mathbb{E}[\cdot]$ is the expectation operator. This implicitly assumes that the EHWSN is designed to meet the request demands such that $\mathbb{E}[d] = \mathbb{E}[h]$. Causality constraints require that the cumulative node energy cannot exceed the cumulative harvested energy i.e., $\sum_0^t z_t \leq \sum_0^t h_t$. The node is operational at time t if $b_t + h_t \geq z_{min}$. Otherwise, there is a *downtime*. When this occurs, the node becomes non-operational and consumes all of the energy harvested to recharge its battery to a user-specified level before starting up again.

One trivial policy may be to greedily maximize conformity at all times, i.e., $k_t^i = 1$. This increases the risks of downtimes due to severe power depletion. Another trivial solution is to always operate the node at the minimum level of operation i.e., $z_t^i = z_{min}^i$. This leads to wastage of the potential utility of the node. The ideal energy management strategy would reduce downtimes while ensuring that all energy harvested is used wisely to maximize utility. The energy-neutrality of the node at time t is given by the Energy Neutral Performance (ENP) metric $e_t = \sum_0^t \mathcal{B}(h_t - z_t) = b_0 - b_t$, expressed as the total difference between harvested and consumed energy [7–9].

The *ENP-utility* is u_t^{ENP} , given by a function $U^{ENP}(e_t)$ which reflects the energy-neutrality of the node. The node-utility is a weighted sum of the individual task-utilities w.r.t. their priorities. For an EHWSN with n -tasks, the relative priorities between its $n + 1$ objectives is expressed by $\omega_t = (\omega_t^1, \omega_t^2, \dots, \omega_t^{n+1})$ where $\omega_t^i \in [0, 1]$ is the priority/preference for the i th objective. $\omega_t^{n+1} = (1 - \sum_{i=1}^n \omega_t^i)$ is the implied priority for the energy-neutrality of the node. With a slight abuse of notation, for single-task EHWSNs, the priorities of task maximization and ENO are represented by ω_t and $(1 - \omega_t)$. The agent's ultimate objective is to maximize the overall node-utility $w_t = \sum_{i=1}^{n+1} u_t^i \omega_t^i$. If the node had infinite energy, the obvious policy would be to maximize u_t^i for all tasks. However, due to severe energy constraints, the MORL agent has to decide *which* utilities to maximize and by *how much* w.r.t. the user's priority.

It is important to note that u_t^i and w_t denote the instantaneous utilities. They do not reflect long-term returns and therefore cannot directly quantify the effectiveness of the *policy*. For instance, in the case of a solar EHWSN, the instantaneous ENP e_t does not give us much information about the long-term energy-neutrality of the policy because it is expected to fluctuate over the course of a day. Thus, to compare and improve policies, we require the notion of the *value of a policy* which we discuss in the following section.

4. Theoretical Background

In this section, we introduce the Deep Deterministic Policy Gradient (DDPG) RL algorithm [59] and describe the MOMDP for MOO using RL.

4.1. Single-Objective RL

In a standard SORL, an agent observes the state of its environment $s_t \in \mathcal{S}$ at each timestep and then performs an action, $a_t \in \mathcal{A}$, in accordance with some policy $\pi(a|s)$. As a result, it moves on to the next state s' and receives a scalar reward r_t reflecting how optimal the action was in relation to the optimization objective. The rewards are presented via the reward function $\mathcal{R}(s, a, s')$ and are typically discounted by $\gamma \in [0, 1]$. The procedure then restarts once the agent achieves a terminal state (the conclusion of an episode). The agent learns progressively better policies that maximize its cumulative reward using the rewards and its prior experiences. An episodic discounted Markov Decision Process (MDP) is used to model this sequential decision-making situation. The MDP is defined by a tuple $(\mathcal{S}, \mathcal{A}, \mathbb{P}, \mathcal{R}, \gamma)$ where \mathcal{S} is the continuous state space, \mathcal{A} is the continuous action space and $\mathbb{P}(s'|s, a)$ defines the transition probability from state s to s' as a result of action a .

The Q-value of a state-action pair $Q^\pi(s, a)$, w.r.t. policy π , gives the *expected* return when executing action a from state s as defined in Equation (1a) for an episode of length T . It can be computed recursively by using the Bellman equation in Equation (1b).

$$Q^\pi(s, a) = \mathbb{E}_\pi \left[\sum_{t=0}^T \gamma^t R(s_t, a_t, s_{t+1}) | s_0 = s, a_0 = a \right] \quad (1a)$$

$$Q^\pi(s, a) = \mathbb{E}_\pi [R(s, a, s') + \gamma Q(s', \pi(s'))] \quad (1b)$$

The main idea behind RL is for the agent to learn a policy to select an action that maximizes the Q-value for each state that it encounters (procedural knowledge). This requires learning the Q-values of all state-action pairs (predictive knowledge). We approximate the Q-values with a neural function approximator $Q_\theta(s, a)$ parameterized by θ (the *critic*). The policy is output by a function $\pi_\phi(s)$ with parameters ϕ (the *actor*).

We employ the Deep Deterministic Policy Gradient (DDPG) [59] RL algorithm for this work. DDPG is an off-policy actor-critic formulation. Off-policy points to the fact that the algorithm can learn the Q-function for a policy π although its training examples may be obtained from a (slightly) different policy. This off-policy behavior will be crucial later on when we have to learn policies with different objectives from the same set of training examples.

Previous RL solutions were limited because they used discrete state-action spaces [7,9]. We opt for DDPG because it supports continuous states and actions. It is also simpler to implement in comparison to other RL algorithms of similar nature for continuous control. The DDPG critic evaluates the Q-value of state-action pairs whereas the actor outputs a deterministic action for a given state. To encourage exploration, some random noise is added to the actor's output during the learning phase. We also maintain time-delayed versions of the actor and critic referred to as *target* networks [15], $Q_{\theta^-}(s, a)$ and $\pi_{\phi^-}(s)$, to increase learning efficiency and stability. The parameters of the target networks are updated by Polyak averaging with the parameters of their main counterparts.

During training, the agent collects experience tuples (s, a, r, s') at each timestep t and stores it in an experience replay buffer [15]. At each training step, a random minibatch \mathbb{B} of experiences are selected and a gradient *descent* is performed to minimize the loss functions in Equations (2a) and (2b).

$$L(\theta, \mathbb{B}) = \mathbb{E}_{\mathbb{B}} [Q_\theta(s, a) - (r + \gamma Q_{\theta^-}(s', \pi_{\phi^-}(s')))] \quad (2a)$$

$$L(\phi, \mathbb{B}) = -\mathbb{E}_{\mathbb{B}} Q_\theta(s', \pi_\phi(s')) \quad (2b)$$

Minimizing Equation (2a) gives more accurate estimates of expected return in taking a particular action in a particular state. On the other hand, minimizing Equation (2b) corresponds to choosing the action that maximizes return (or Q-value) from a given state.

4.2. Multi-Objective RL

In a typical MOO problem, an optimizing variable is mapped into a multi-dimensional objective space by *objective functions*. Pareto-optimal points are those mappings in which one objective's value cannot be increased without lowering the value of at least one other objective. The utility corresponding to the value of the optimizing variable is given by the linear combination of its mapped objective values weighted by user-defined priorities (We do not cover non-linear utility functions in this work).

Most popular MOO solutions assume a time-invariant objective function. In such a case, Evolutionary Algorithms (EA) or Monte Carlo (MC) rollouts are used to map a sample population of the optimizing variable to points in the objective space. This usually takes many rollouts/generations. By doing so, we hope to either find the value of the variable that has the highest utility or approximate the Pareto-frontier with some function or visualization technique. These methods have been used extensively in the optimal positioning of sensor networks which involves a tradeoff between the conflicting objectives of node lifetime, coverage, and cost within the computation, energy, and communication constraints [67]. For e.g., in [71], the authors use GA to minimize energy consumption and node count while maximizing coverage for a sensor network. They assume that the nodes are statically deployed and that the Quality of Service (QoS) remains constant. Each optimization process takes hundreds of generations to converge. This approach works for this particular problem because the working environment (optimization space) does not vary drastically from one generation to another i.e., the optimization problem is time-invariant.

Unfortunately, these methods are not very useful when the objective function is *time-variant* like in the case of energy optimization of EHWSNs with variable energy availability at each time step. In our case, the RL agent has to output an action at every timestep such that it trades off between the different objectives. The agent's action $\pi(s) = a$ is the optimizing variable in this case. The objective functions are the Q-functions $Q^\pi(s, a)$ because they quantify how the actions will ultimately affect the long-term cumulative payoff. $Q^\pi(s, a) = Q^\pi(s, \pi(s))$, however, is parameterized by the state s , which evolves at every timestep. Figure 3 illustrates this, showing how the same set of sampled actions map to different locations in the objective space as the state changes from s_1 (blue) to s_2 (orange). Thus, due to the time-varying nature of the objective space, using elitist multi-objective optimization techniques like Monte Carlo (MC) rollouts or Evolutionary Algorithms (EA) is particularly unfeasible. If one were to use, say MC, one would have to sample many rollouts, approximate the Pareto frontier, and find the solution with the best utility at *every time step*. This requires very fast and very powerful computation which is not possible in sensor nodes or similar embedded systems.

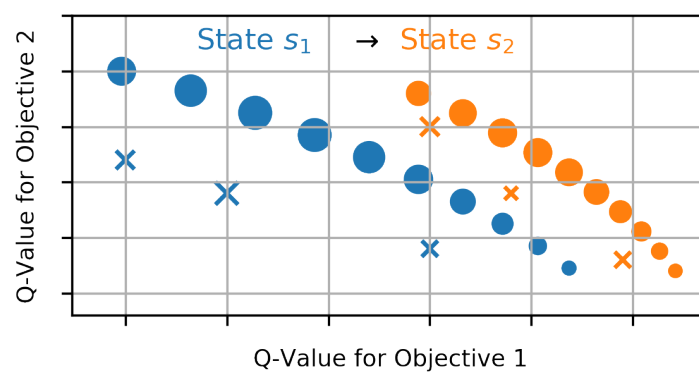


Figure 3. The Pareto-front changes when the agent transitions from state s_1 to s_2 . Crosses indicate Pareto-dominated actions. The marker size represents the utility of the action.

Thus, we propose a MORL framework in Section 5. Our framework learns the Q-functions and policies that can deduce the best action to maximize utility from Pareto-frontier. We first develop a general Multi-Objective Markov Decision Process (MOMDP) for MORL with m objectives. \mathcal{S} is the continuous state space, and \mathcal{A} is the continuous action space. The reward function is now a vector function, $\vec{R}(s, a) = [R_1(s, a), R_2(s, a), \dots, R_m(s, a)]$ and the discount factors corresponding to different objectives are given by $\gamma = [\gamma_1, \gamma_2, \dots, \gamma_m]$. The transition probability from s to s' due to action a is given by $\mathbb{P}(s'|s, a)$. The Q-function is also a vector function $\vec{Q}^\mu = [Q_1, Q_2, \dots, Q_m]$ whose elements represent the different objective functions. μ is the MORL policy that extracts the Pareto-optimal action w.r.t. the user-preference $\omega \in \Omega$. The next section describes how we create a suitable MOMDP for EHWSNs and how the agents can learn the vector Q-functions to extract the optimal actions. Ω determines the space of preferences among the m objectives. The MORL policy μ is now associated with an m -dimensional vector Q-value function $\vec{Q}^\mu = [Q_1, Q_2, \dots, Q_m]$ whose components correspond to the different objective functions. μ extracts the Pareto-optimal action w.r.t. the user-preference $\omega \in \Omega$. In the following section, we develop a suitable MOMDP for EHWSNs and present solutions to learn the vector Q-functions and extract the optimal actions.

5. Proposed MORL Framework

5.1. MOMDP Formulation

Here we define the reward function and the state-action space of our MOMDP for the system model in Section 3. Although the following description is specific to the energy-scheduling problem in EHWSNs, the general idea behind the MOMDP formulation is applicable for any type of resource-scheduling problem in IoT embedded systems.

Multiple Reward Functions: Since modern EHWSNs have multiple objectives, a reward function that supports multiple sources of rewards is needed. In previous methods where multiple objectives are projected into a scalar by scalarization, the rewards become noisy and obfuscate the actual objectives. The biggest downside is that tradeoffs cannot be made at runtime [51] because the relative weights between objectives need to be known and fixed before training. Another drawback is that scalarization sometimes involves intricate reward shaping which introduces considerable design bias [7,52,72]. Our framework learns from distinct, independent reward signals to get around these restrictions without any complex reward shaping. Each of these reward signals represents a single optimization target. In our framework, the task rewards are the task utilities, and the ENP reward is the ENP-utility.

Well-defined state space: Our framework defines the state at time t by a tuple $s_t = (\tau, b_t, \bar{b}_t, h_t, f_t, d_t)$. $d_t = (d_t^1, d_t^2, \dots, d_t^n)$ is a tuple containing the different task requests and h_t is the harvested energy. Our state definition includes important temporal information (which are not present in previous works)—(i) τ which represents the time of the day, (ii) $\bar{b}_t = \sum_{k=0}^T b_{t-k} / T$ which is a moving average of battery values over a horizon T , and (iii) $f_t \in [0, 1]$ which is a rough prediction of future energy supply as in [9]. By making these additions to the state definition, the learning process is stable and faster compared to earlier research [7,50].

Safe Actions: RL learns through exploration and mistakes are inevitably necessary during the initial stages of training. These mistakes need to be minimized in the real world because they lead to loss of utility and may have potentially unintended consequences, e.g., node shutdown due to energy depletion. Previous RL formulations define actions so that they directly correspond to the energy consumption of the node, e.g., the node duty cycle or the transmission power [7,9,10,44,50]. This is dangerous because the agent may sometimes sporadically take very unreasonable actions (e.g., duty cycles suddenly spike causing battery exhaustion). This is usually due to maximization bias in Q-learning when using a discrete action space or defective policies owing to factors such as bad experience samples and learning instability.

In our formulation, we define the action to be the node's conformity to various task demands. For an n -task EHWSN, the action is $k_t = (k_t^1, k_t^2, \dots, k_t^n)$ where k_t^i is the conformity of the node to the request d_t^i . This definition states that actions are *safe* because they never over-provision energy and hence avoid unintended battery depletion. As a result, the definition of our actions reduces the effects of catastrophic policies even if learning results in a bad policy, in contrast to action definitions in earlier techniques [7,9,50].

5.2. Runtime MORL

We now describe our first algorithm, *Runtime MORL* (Algorithm 1). This algorithm takes SORL actor-critic pairs trained with different reward functions as input. Each of these actor-critic pairs is trained to maximize a different objective. The algorithm uses these actor-critic pairs and generates a policy that can tradeoff between different objectives at runtime without additional training.

The action space of n -task EHWSN has $|k| = n$ dimensions. However, the EHWSN has to optimize across $n + 1$ objectives, with energy neutrality as the $n + 1$ th objective. Algorithm 1 outputs each element of the action space using n pre-trained greedy actor-critic networks (π_i, Q_i) . The i th task's greedy conformance g_i , is output by π_i . The *total conformance* of the node g_{ENP} , with respect to the *total demand* $d = \sum_{i=1}^n d^i$, is output by another pre-trained greedy actor-critic (π_{ENP}, Q_{ENP}) . All greedily energy-neutral actions can be represented by a plane $g_{ENP} = \sum_{i=1}^n k_i$, in the action space. The convex hull that contains this plane and all of the greedy actions is then determined.

Minimizing Computation Costs

One solution to finding the optimal action k^* would be to learn a function that maps the entire convex hull to the objective space and then maximizes the node-utility using methods like gradient descent. This makes the learning problem very complex with extremely high computation and learning costs. Another solution would be to maintain a *set* of policies for each preference (ω) but this is not a sustainable approach because ω takes continuous values. In Algorithm 1, we *sample* the locally approximate Pareto-optimal from the convex hull to determine the optimal action k^* . Algorithm 1 samples j actions x_1, x_2, \dots, x_j according to the user-preference $\omega = (\omega_1, \omega_2, \dots, \omega_{ENP})$. The core idea behind this approach is that when we progress from one greedy action to another along the convex hull, we are actually moving along the Pareto-front in the objective space and trading off between different objectives. This is possible in our case because we have assumed task-utility functions are a monotonically non-decreasing function of conformity (or action). The linear combination of the critics' outputs Q_i and Q_{ENP} , weighted by the task preferences ω_i and ω_{ENP} , gives us the composite Q-values for each of these sampled actions. The action with the highest values is the most locally optimal action. When using Algorithm 1 in this way to determine the optimal action, a change in ω at *runtime* merely necessitates inferring the critics and recalculating the action-values, which is a relatively inexpensive process compared to gradient descent. By sampling more actions, we can increase the optimality of the solution with a corresponding increase in computation costs. Overall, compared to doing gradient descent to determine the best action, this technique uses far less processing. With this sampling strategy, we can always identify an action that is at least as beneficial as the greedy ones without making any assumptions about the concavity of the Pareto-frontier. This is important because concave Pareto-frontiers are a challenging problem for several MORL algorithms.

The implementation of Algorithm 1 for a scenario with a single-task optimization is shown in Figure 4. While g_{ENP} greedily preserves energy-neutrality by decreasing the conformity k , g_1 greedily maximizes the task-utility by boosting conformity. Here, g_1 and g_{ENP} define a straight line which is the convex hull. Two points on the line denoted by the red crosses are sampled using Algorithm 1. The outputs of the critics (Q_1, Q_{ENP}) are used to map the Q-values corresponding to all actions (both greedy and sampled) onto the objective space. These Q-values are weighted by ω and the best action is determined.

In Figure 4, action x_1 is the best action since it has the highest composite Q-value (indicated by the size of the circles).

Algorithm 1: Runtime MORL.

Input : $\omega \in \Omega$, priorities for $n + 1$ objectives
 $s \in \mathcal{S}$, State
 (Q_i, π_i) , Greedy actor-critics, $i = 1, 2, \dots, n$
 (Q_{ENP}, π_{ENP}) , Energy-neutral actor-critic

Output: Action k^* that maximizes utility, $|k^*| = n$

```

1  $actionList = []$  // Proposed actions list
2 for  $i = 1, 2, \dots, n, ENP$  do
3    $g_i = \pi_i(s)$  // Greedy Actions
4    $actionList.append(g_i)$ 
5 end for
6 Sample  $j$  actions  $x_1, x_2, \dots, x_j$  from the convex hull of actions in  $actionList$  and
  append to  $actionList$ 
7  $W = \{ \}$ 
8 for  $x$  in  $actionList$  do
9    $W[x] = \sum_{i=1}^{n+1} Q_i(s, x)\omega^i$ 
10 end for
Return :  $k^* = \underset{x}{\operatorname{argmax}} W[x]$ 

```

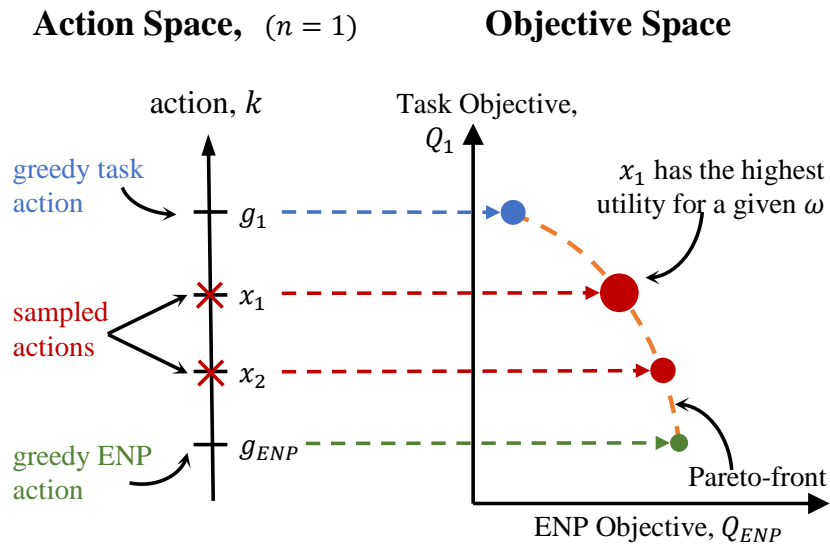


Figure 4. As we move from one greedy action to another in the action space, we traverse along the Pareto-optimal frontier in the objective space. *Runtime MORL* samples actions (red crosses) from in between the greedy actions, g_1 and g_{ENP} .

5.3. MORL with Off-Policy Corrections

Now, let us focus on the scenario where there are no pre-trained, greedy actors and critics available; and greedy actors/critics have to be trained tabula rasa. With our second algorithm, *Off-policy MORL* (Algorithm 2), the critics learn their Q-values from the experience samples gathered from the agent's interaction with the environment, while the actors simultaneously learn the greedy policies. Using Algorithm 1, the agent chooses actions that fall between the greedy actions based on the preference ω parameter. Thus, when implementing Algorithm 2, the critics must learn the Q-values Q_i for a greedy policy π_i from transitions generated by a different policy, say μ . This requires *off-policy corrections* i.e., a method to compensate for the difference in state transition probabilities (s to s') between π_i and μ . We achieve this by multiplying the expected Q-values of the next state

by their ratio of their transition probabilities, $\rho_i(s, s') = \frac{\mathbb{P}(s'|s, \pi_i)}{\mathbb{P}(s'|s, \mu)}$ in Equation (3) where we use the approximation $\rho_i(s, s') \approx \omega_i$. This approximation makes sense (theoretical guarantees are not in the scope of this work) because μ is increasingly dominated by π_i when ω_i is closer to unity and therefore does not significantly alter the expectation. However, when ω_i is extremely low, μ is considerably further away from π_i and as a result, the expected return is proportionately decreased.

$$\begin{aligned} Q_i(s, a) &= \mathbb{E}_{\pi_i}[r^i + \gamma_i Q_i(s', \pi_i(s'))] \\ &= \mathbb{E}_{\mu}[r^i] + \gamma_i \rho_i(s, s') \mathbb{E}_{\mu}[Q_i(s', \pi_i(s'))] \\ &\approx \mathbb{E}_{\mu}[r^i + \gamma_i \omega^i Q_i(s', \pi_i(s'))] \end{aligned} \quad (3)$$

Algorithm 2: Off-policy MORL.

Input : γ_i , discount factor for i th objective, $i = 1, 2, \dots, n + 1$
Initialize: Randomly initialize actor-critic pairs (Q_i, π_i) and empty replay buffer D

```

1 for episode = 1,  $L$  do
2   for  $t = 1, T$  do                                     //  $T$  = episode length
3     Observe the preferences  $\omega_t \in \Omega$ 
4     Observe state  $s_t$ 
5     Select action  $a_t$  using Algorithm 1
6     Execute action  $a_t$ , observe the reward vector  $\vec{r}_t = [r_t^1, r_t^2, \dots, r_t^m]$  and the
       next state  $s_{t+1}$ 
7     Store  $(s_t, a_t, \vec{r}_t, s_{t+1}, \omega_t)$  in  $D$ 
8     Sample minibatch  $\mathbb{B}$  of  $N$  transitions from  $D$ 
9     for  $i = 1, n + 1$  do
10      Update  $Q_i$  using  $r_i$  and  $\gamma_i$  with Equation (3),
11      Update  $\pi_i$ 
12    end for
13  end for
14 end for

```

6. Evaluation Setup

6.1. Simulation Environment

We test our framework by simulating solar EHWSN systems using data on solar radiation collected hourly by external rooftop pyranometers from 1995 to 2014 [73]. As a result, we chose an hour as the time interval for each timestep. We train the RL agents for the first ten years (1995–2004), and then measure their effectiveness over the following ten years (2005–2014). Each episode of our MDP lasts for one day (or 24 timesteps). The ten-year training period can be shortened to less than a year if we increase the granularity of the timesteps and adjust the discounting rates correspondingly. However, we maintain an hourly resolution for a fair comparison with previous methods [8,9]. An episode abruptly terminates with zero rewards when downtime occurs. In such a case, a new episode begins once the node has recovered. The parameters of the evaluated EHWSN system, normalized to b_{max} , are shown in Table 1. When $h_t = 0$ (no harvested energy), the node can deplete 5% of the battery per timestep. This means that the node can drain a fully charged battery within 20 h at maximum power and takes 200 h (≈ 8 days) at minimum power with no energy harvesting. These parameters are based on a realistic EHWSN [74] with a current rating of 100 mA equipped with a 2000 mA h battery. As soon as the battery capacity falls below 10%, the node enters recovery mode and is reset. To simplify comparison and analysis, we assume this recovery is instantaneous without loss of generality. The request function generates the task demands (or requests) at random so that $\mathbb{E}[h_t] \approx \mathbb{E}[d_t]$. This guarantees that ENO is indeed achievable. The rolling average of h_t for the following

10 days is added with some random noise to provide a rough estimate of the weather forecast f_t .

Table 1. Simulation Parameters.

Parameter	Maximum Value	Minimum Value
Battery, b_t	b_{max}	$b_{min} = 10\%$ of b_{max}
Harvester, h_t	$h_{max} = 5\%$ of b_{max}	$h_{min} = 0$
EHWSN, z_t	$z_{max} = 5\%$ of b_{max}	$z_{min} = 0.5\%$ of b_{max}
Requests, d_t	$d_{max} = 5\%$ of b_{max}	$d_{min} = 0.5\%$ of b_{max}

6.2. Utilities and Reward Functions

We use single-task (bi-objective) and dual-task (tri-objective) EHWSNs for our evaluations. The single-task node increases the node conformity linearly in compliance with the user demand while retaining long-term energy neutrality to maximize sense-utility [9,18,20,29]. Thus, we establish the rewards for maximizing the sensing rate by the sense-utility u_t^{sense} , which increases linearly with conformity (energy usage) in accordance with the *linear-utility* function in Figure 5 (left).

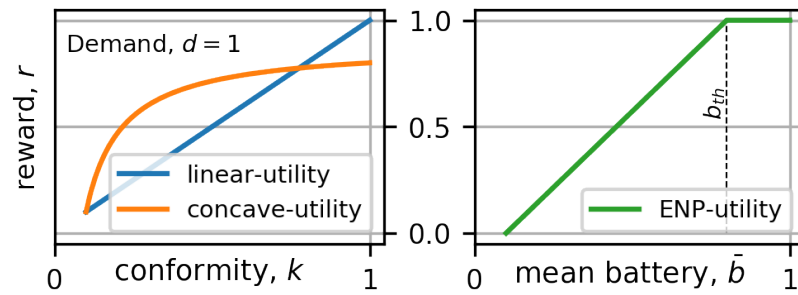


Figure 5. Linear and concave reward functions quantify the utilities for different tasks such as sensing, communication, and processing. The ENP-utility function indicates the long-term energy neutrality of the node.

The ENP-utility u_t^{ENP} corresponds to the rewards that represent the energy-neutrality of the node given by

$$u_t^{ENP} = \begin{cases} 1, & \text{if } \bar{b}_t \geq b_{th} \\ \frac{\bar{b}_t - b_{min}}{b_{th} - b_{min}}, & \text{otherwise} \end{cases} \quad (4)$$

Figure 5 (right) illustrates this reward function. b_{th} is a user-defined battery threshold, and \bar{b}_t is the moving average battery level over ten days. This reward function is similar to those in [7–9,52], but require less reward shaping. In addition, our reward function uses \bar{b}_t instead of b_t since it correctly captures the long-term temporal nature of ENO. b_{th} is fixed at 80% of b_{max} although this can be changed as needed. The relative preference between optimizing sense-utility and ENP-utility is reflected in ω for single-task EHWSN. $\omega = 0$ places an emphasis on energy-neutrality whereas $\omega = 1$ maximizes sense-utility.

We evaluate EHWSN systems that need to sense *and* transmit data when discussing dual-task EHWSNs. These nodes must increase their throughput in addition to maintaining energy neutrality and increasing their sense-utility. We assume a simplified transmission model with Binary Phase Shift Keying (BPSK) modulation with additive white Gaussian noise and Rayleigh fading. This is only for the sake of an example and can be modified as required. We do not consider the effects of multi-hop transmission and routing issues here because it adds another layer of complexity that does not directly pertain to the issue

of MOO. For the sake of simplicity, we have assumed that a receiver is always ready to receive the data.

The node's transmission throughput P is given by Shannon's capacity formula $P = \log(1 + k)$ where k is the SNR of the transmission signal. In our case, the conformity $k = z/d$ is the SNR. The transmission task demand d can be interpreted as the amount of transmission power required to overcome channel noise and maintain the QoS determined by the user and z is the actual transmission power which results in throughput P . $u_t^{tx} = P$ is both the task-utility and reward. Higher SNR is necessary for higher throughput, but throughput does not increase linearly with higher SNR (transmission power). The concave-utility reward function in Figure 5 serves as a representation of this relationship.

Since the utility is non-linear, it may be wiser to use transmission energy to drastically improve the throughput when the channel is very noisy (\sim high demand) than to use the same amount of energy to increase the throughput by only a small amount when there is less noise (\sim low demand).

The dual-task node must constantly choose how much energy to devote to transmission and sensing operations in order to increase throughput (or tx-utility) u_t^{tx} and sense-utility u_t^{sense} while maintaining long-term ENO (maximizing u_t^{ENP}). The tuple $\omega = (\omega_{sense}, \omega_{tx}, \omega_{ENP})$ s.t. $\omega_{ENP} = 1 - (\omega_{sense} + \omega_{tx})$ indicates the relative preference between the objectives.

6.3. Metrics

We compare the *task-utilities* of various solutions based on their yearly average. The total number of times the node enters recovery mode (i.e., downtimes) is used to compare the *energy-neutrality* of various solutions. Using downtimes as a metric for ENO is a more accurate reflection of the actual energy-neutrality than the ENP-utility and facilitates fair comparison. An intelligent policy strikes an equilibrium between increasing task utilities and reducing downtimes. The *learning cost* for a particular policy is determined by the number of downtimes that occur during the training period, with fewer downtimes being preferable (the training duration is the same for all RL agents). The node should ideally learn an energy management strategy with as little downtime as is feasible.

We perform each experiment with ten random seeds and average over them for comparison. The interquartile range (IQR) is indicated by the shaded regions and error bars (not shown in some figures for clarity).

7. Experimental Results

In this section, we present our results and answer the following questions:

- Do RL agents trained using the MDP (state and action definitions) based on our proposed general MORL framework perform better than heuristic methods and traditional RL solutions when optimizing for a single objective? Specifically, do they extract higher utility at lower learning costs?
- How well does the proposed Algorithm 1 tradeoff between multiple objectives at *runtime* using greedy SORL agents? How does it compare to traditional scalarization methods that are optimized using non-causal information?
- Can the MORL agents trained with our proposed MOMDP learn policies to maximize the tradeoff between different objectives? What is the cost of training in such a scenario?

A summary of the different SORL and MORL agents we evaluate is given in Tables 2 and 3.

Table 2. Single-Objective ENO Agents.

	<i>Sense Objective,</i> $\omega = 1$	<i>ENP Objective,</i> $\omega = 0$
Ours (RL Agents)	<i>sense</i>	<i>enp</i>
Ours (Smaller NNs)	<i>tiny_sense</i>	<i>tiny_enp</i>
Heuristic Methods	<i>max_enp</i>	<i>max_k</i>
Partially Markov States [7,9,10,44,50]		<i>pomdp_enp</i>
Absolute Actions [7,9,10,44,50]	<i>raw_sense</i>	<i>raw_enp</i>

Table 3. Multi-Objective ENO Agents.

Method	Name	Rewards/Values
Ours (Algorithm 1)	<i>morl_runtime</i> (2-task)	$\omega Q^{\pi_{sense}} + (1 - \omega) Q^{\pi_{enp}}$
Ours (Algorithm 2)	<i>morl_offpolicy</i> (2-task)	$\omega Q^{\pi_{sense}} + (1 - \omega) Q^{\pi_{enp}}$
Ours (Algorithm 2)	<i>morl_multi</i> (3-task)	$\omega_{sense} Q^{\pi_{sense}} + \omega_{tx} Q^{\pi_{tx}} + \omega_{ENP} Q^{\pi_{enp}}$
Scalar Product [7,50,52]	<i>mul_scalar</i>	$u^{sense} \times u^{ENP}$
Scalar Sum [51,52]	<i>add_scalar</i>	$\omega u^{sense} + (1 - \omega) u^{ENP}$

7.1. Single-Objective RL Policies Using Proposed MDP

7.1.1. Comparison with Heuristic Methods

Figure 6 shows the sense-utility and the corresponding downtimes experienced by the sensor nodes for a test period from 2005 to 2014 (ten years) under different policies. *sense* (red) and *enp* (green) are SORL agent policies ($\gamma = 0.997$) that maximize sense-utility and ENP-utility respectively. We compare them with two heuristic policies, *max_enp* and *max_k*.

max_k represents the upper limit of utility maximization. It greedily maximizes the sense-utility using a trivial policy that always conforms maximally ($k_t = 1$) to all task requests without any consideration for long-term energy neutrality. As a result, it is also the least energy neutral with the highest number of downtimes. *max_enp* has the fewest possible downtimes and is, therefore, the most energy-neutral policy. It achieves this by increasing the node conformity with the battery level w.r.t. a non-linear function (shown in Figure 7). Greedy search and non-causal data were necessary to empirically establish the parameters of this function. *max_enp* indicates the upper limit of ENO because no policy can extract more utility than it does without increasing the frequency of downtimes.

In Figure 6, we observe that the energy neutrality (downtimes) of *enp* and *max_enp* are similar (green and blue bars). This means that *enp* is near-optimal w.r.t. the ENO objective. Using our MDP, *enp* performs as good as *max_enp* without the need for any non-causal information or empirical hand-tuning. Thus, we use *enp* as the baseline for ENO when comparing it with other RL agents. An RL agent would outperform *enp* if it has lower downtimes than *enp* and extracts higher sense-utility.

We also observe that *sense* is more aggressive than *enp* in maximizing utility. *sense* scores higher sense-utility than *enp* at the cost of larger downtimes. This is expected because *sense* was trained using only the sense-utility reward function and does not receive any direct feedback from the ENP-utility reward function. In spite of this, *sense* does not disregard energy neutrality like the trivial *max_k* agent which incurs very high downtimes (orange bars). *sense* learns to avoid downtimes so that it does not lose any opportunity to collect more rewards in the long term. This behavior is attributed to the discounting factor γ , which indirectly accounts for the ENO objective. We cannot conclude *sense* is optimal despite the fact that it extracts higher utility within competitive bounds of energy neutrality. A better solution would increase sense-utility while keeping *sense*'s downtimes

constant. Since it is difficult to establish clear upper bounds in this situation, we compare other agents' sense-utility against *sense* as a starting point.

Figure 8 illustrates the difference between the policies of *sense* and *enp* in more detail with their corresponding battery traces. The time interval shown corresponds to autumn/winter in Tokyo. It is very difficult to avoid downtimes during this period because opportunities to recoup any energy losses are very rare as the winter solstice approaches (Day 356). In fact, it is very difficult to avoid downtimes unless the node has full battery reserves on Day 260 and operates at its minimum duty cycle as much as possible. Consequently, *sense*, which is more aggressive in maximizing the duty cycle, experiences a downtime on Day 303 while *enp* maintains a conservative policy and passes the winter with no downtimes. After the winter solstice, both agents start to refill their battery reserves.

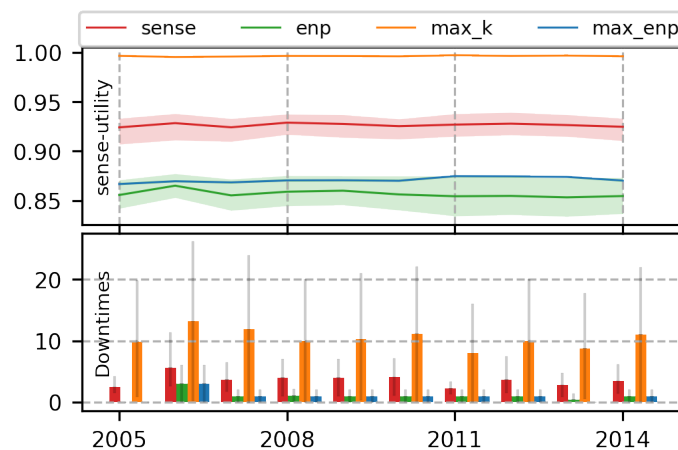


Figure 6. Agent *enp* (ours, green) has similar energy neutrality (downtimes) as the most energy-neutral policy *max_enp*. *sense* (ours, red) sacrifices some of its energy neutrality to increase its utility but is more energy neutral than *max_k*.

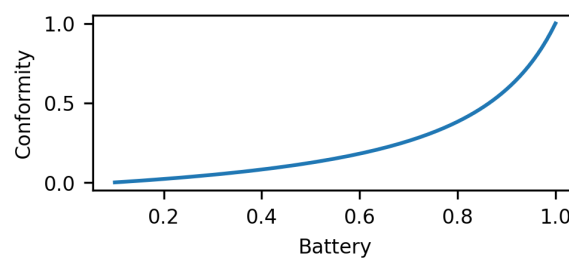


Figure 7. *max_enp* Heuristic Policy. The conformity of the node decreases gradually as the battery depletes.

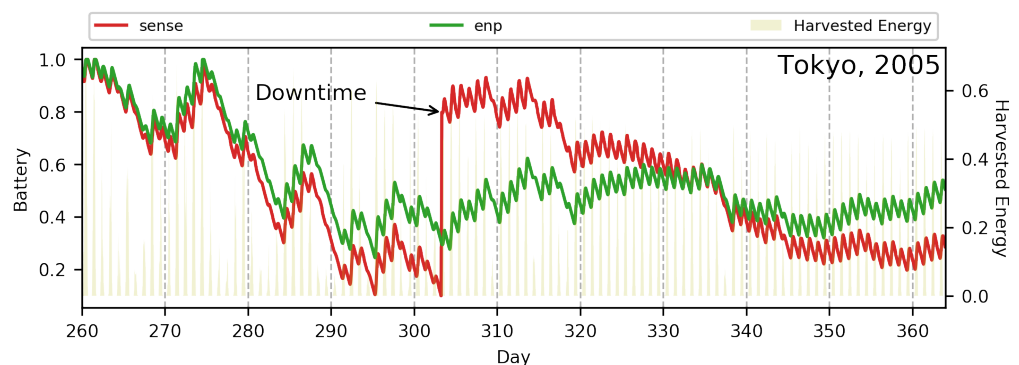


Figure 8. Battery traces for *sense*, *enp*. *sense* is more aggressive than *enp* when maximizing the sense-utility and therefore experiences downtime during winter. The sharp rise in battery level after a downtime signifies a node reset.

7.1.2. Adaptive Nature of RL Policies

RL solutions are superior to heuristic methods because they can adapt to changes in the working environment. Adapting policies to battery inefficiencies has been demonstrated in our previous works [8,9] using a simple model where these inefficiencies were lumped as increased node consumption. In this work, we use a more sophisticated battery model ($\mathcal{B}()$ described in Section 3) that addresses the discrepancies in the charging and discharging efficiencies of the battery and the role it plays during the optimization of energy scheduling.

To investigate the effect of imperfect batteries in our framework, we compare the performance of *sense* with *bad_batt* in Figures 9 and 10. *bad_batt* agent (purple) was trained and tested similarly to *sense* except that its battery charging efficiency was set to 50%. Figure 9 shows the battery traces and duty cycles for *sense*, *enp* and *bad_batt* in the beginning of the year when the days are shorter and so the solar energy is limited. *enp* consistently operates at the minimum duty cycle to conserve energy and avoid downtimes. *sense* tries to maximize the duty cycles during the night depending on how much is harvested during the day. Since *sense* has a perfect battery and there are no losses in storing and retrieving energy, it can play safe and choose to delay the maximization opportunities. On the other hand, *bad_batt* maximizes duty cycles mostly during the day. This way the energy from the solar panel can be directly fed into the node and energy losses due to battery charging and discharging can be minimized. Thus we see that the same MDP can learn very different policies to optimize different objectives and adapt to different working environments. This strengthens the case for using RL methods instead of heuristics for self-adaptive autonomous IoT embedded systems.

We also note that *bad_batt* is almost as optimal as *sense* in spite of its inefficiency (Figure 10). In fact, *bad_batt* seems to have better overall performance than *sense* with higher utility and lower downtimes. However, *bad_batt* has fewer stable policies than *sense* as evidenced by higher variations in performance (wider IQRs) among the ten different seeds that were evaluated. Thus, the presence of an inefficient battery may cause RL to learn policies that are more aggressive in maximizing utilities at the expense of the stability.

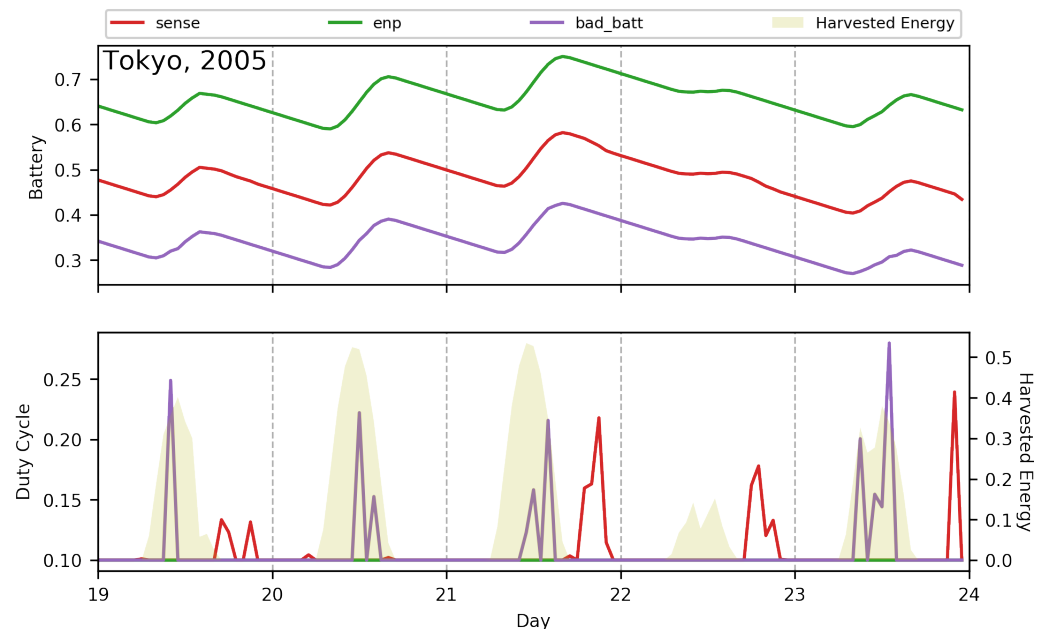


Figure 9. *bad_batt* learns to accommodate for battery inefficiencies by maximizing duty cycles during the day. *sense* maximizes its duty cycle during the night depending on how much energy it was able to harvest during the day.

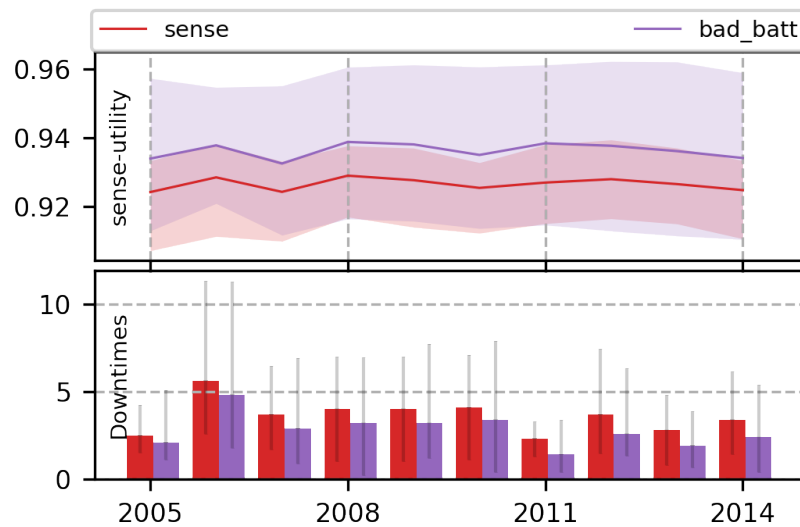


Figure 10. SORL methods can adapt to changes in working parameters.

7.1.3. Superiority of Proposed MDP Formulation

Inclusion of temporal information for long-term optimization: The MDPs of previous methods [7–10,40,50] did not include sufficient temporal information in their state definitions i.e., the states were only partially observed. This resulted in unstable policies as well as larger learning costs. To study the effect of partially Markov states, we designate an agent as *pomdp_enp* that has omitted τ and \bar{b} from its state definitions ($s_t = (h_t, f_t, b_t, d_t)$) and is trained to maximize ENP-utility using the same reward function and training environment as *enp*.

Since both *enp* and *pomdp_enp* are maximizing ENP, we are interested in how many downtimes they incur during learning and testing. Figure 11 compares the learning costs (top figure) and the test performance (bottom figure) between *enp* and *pomdp_enp*. We observe that *enp* (green) has lower learning costs than *pomdp_enp* (purple), which totals to approximately a 15% reduction. We also observe from the test results (bottom figure) that *enp* is also more energy neutral than *pomdp_enp*.

pomdp_enp is less optimal than *enp* because it does not have access to sufficient temporal information. This results in aliasing between different states. The result of such state aliasing is shown in Figure 12 which shows the battery and node energy traces for *enp* and *pomdp_enp*. At the beginning of Day 81, both agents are in the same state. However, *pomdp_enp* observes its state as only by the instantaneous values of (h_t, f_t, b_t, d_t) whereas *enp* observes its state with additional temporal information: τ which represents the time of the day and $\bar{b}_t = \sum_{k=0}^T b_{t-k} / T$ which is a moving average of its past battery values.

enp which has access to temporal information learns that it is okay to maximize duty cycles at dawn (because future energy harvesting possibilities will be available soon) but not at dusk (when there will be no chance of harvesting for a long period of time). We can observe this as the green spikes that occur at the beginning of the day (bottom figure). However, as far as *pomdp_enp* is concerned, the states before sunrise and the states after sunsets are the same because no energy is being harvested. So it (wrongly) learns to maximize the energy consumption both at dawn and dusk (purple spikes when there is no energy being harvested). This results in a very poor policy that has high learning costs.

Thus, we can see that sufficient temporal information is necessary to optimize for long-term ENO. Thus, our proposed MDP state definitions with sufficient temporal information enable learning more optimal policies at much lower costs. We also observe that the exclusion of temporal information does not affect the performance when maximizing sensing-utility (not shown). This is expected because optimizing policies with long foresight are not very important for sense-utility maximization.

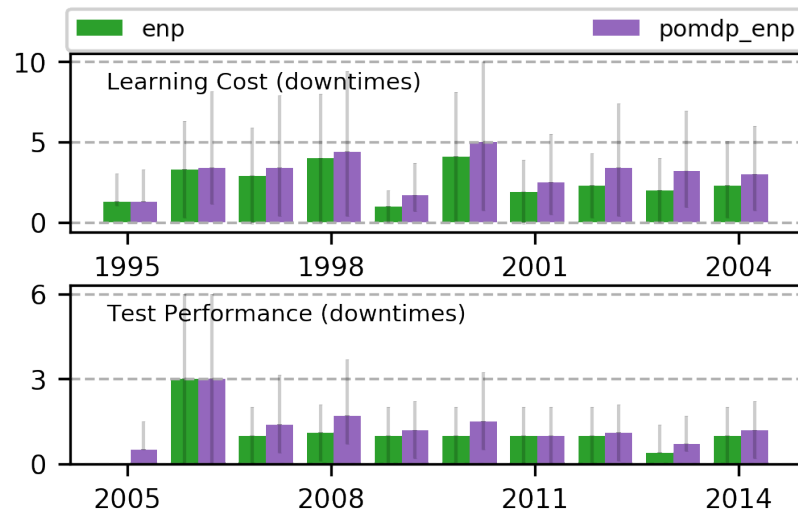


Figure 11. Including temporal information in the state definition of *enp* (ours) decreases the downtimes during learning as compared to *pomdp_enp* (traditional MDPs).

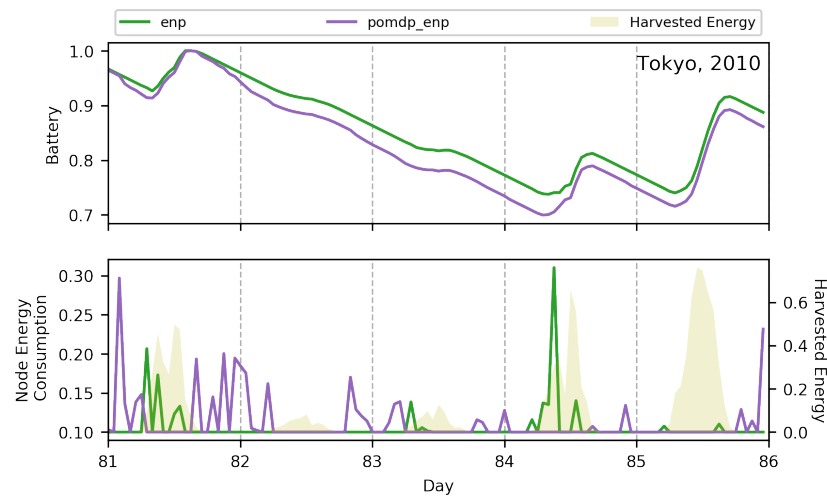


Figure 12. *enp* (ours) learns to discriminate between aliased states using temporal information.

Safer action definitions for efficient learning: In [29], the authors make the case that the utilities of the task vary with time and user requirements. They argue that it is more desirable to expend energy when the utility of the task is higher for the user than when the utility is low. Traditional RL methods did not take this time-varying utility of tasks into account and thus were not very energy efficient. One solution would be to include the user's task demand d_t , into the state definition but our preliminary results show that this requires much more computation and is less stable when training. In our MDP, we propose to define actions as the conformity k_t of the sensor node to the task demand d_t . This accommodates the time-varying nature of utility without an increasing problem complexity.

Another major advantage of our action definition is that it is much "safer". Traditional methods defined the MDP actions as z_t , i.e., the amount of energy allocated to be consumed by the node at each timestep [7–10,40,50]. These action definitions led to high learning costs due to "catastrophic mistakes". For e.g., during the exploration phase, there is nothing stopping an agent from driving the node at a very high duty cycle even when there is not enough energy available. This leads to node shutdown (downtime) which is very undesirable because we would like our nodes to be at least operational, albeit non-optimally, during the learning phase. After committing many such mistakes, the node learns to avoid downtimes but this raises the learning costs. With our action definition,

even when the node explores using high conformity actions, the actual energy expended never exceeds the demand and is always *relative* to the demand. This forms a natural check against unnecessarily high energy usage and dangerous duty cycles thus minimizing downtimes and unsafe exploration.

We evaluate agents *raw_sense* and *raw_enp* and compare them with *sense* and *enp* to study the effects of action definitions during learning and testing. *raw_sense* and *raw_enp* are identical to *sense* and *enp* except that their actions are defined as the absolute allocated energy z_t . *sense* and *enp* define their actions as the conformity k_t .

In Figure 13 (bottom), we observe that our RL agents, *sense* (red) and *enp* (green), incur significantly less downtimes during learning compared to agents using traditional action definitions *raw_sense*(orange) and *raw_enp*(blue). This is especially true during the early training phase. For e.g., in the year 1995, the learning cost of *raw_sense* (orange bar) is extremely high even though it extracts much less sense-utility than *sense* (red). This is because the actions of *sense* are defined relative to the demand and therefore never over-provisions energy. This stops the node from exploring unnecessary and dangerous states. This is important during training because “bad” experiences can not only increase downtimes but also reduce the training stability. This is clearly observed in *raw_sense* (orange bar) also suffers from high IQR (which indicates unstable learning) as a result of inefficient learning. We observe that our action definition decreases downtimes by approximately 70% for both *sense* and *enp* w.r.t. *raw_sense* and *raw_enp*.

We also observe that the policies learned by *raw_sense* and *raw_enp* are inferior to *sense* and *enp* in Figure 14. When we compare *enp* and *raw_enp*, we observe that *enp* extracts much higher utilities than *raw_enp* although they have similar downtimes. This means *raw_enp* is losing out on many opportunities in maximizing utility. It is also very obvious that *raw_sense* is non-optimal. Although its downtimes are almost as high as that of *sense*, its utility maximization is much inferior to that of *sense* by a large margin. Thus, by defining MDP actions in a relative manner, the nodes can learn much better policies that incorporate the time-varying utility of tasks and reduce the learning costs dramatically.

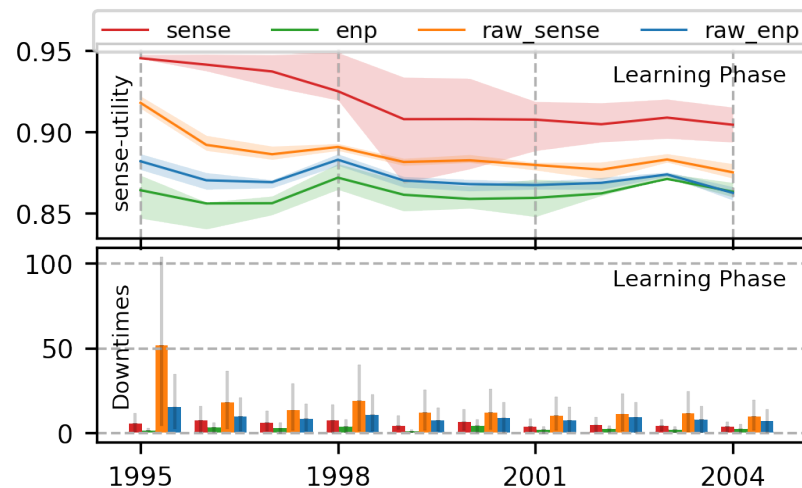


Figure 13. Our safe action definition (*sense* and *enp*) prevents over-provisioning and reduces the learning costs compared to traditional MDP definitions (*raw_sense* and *raw_enp*).

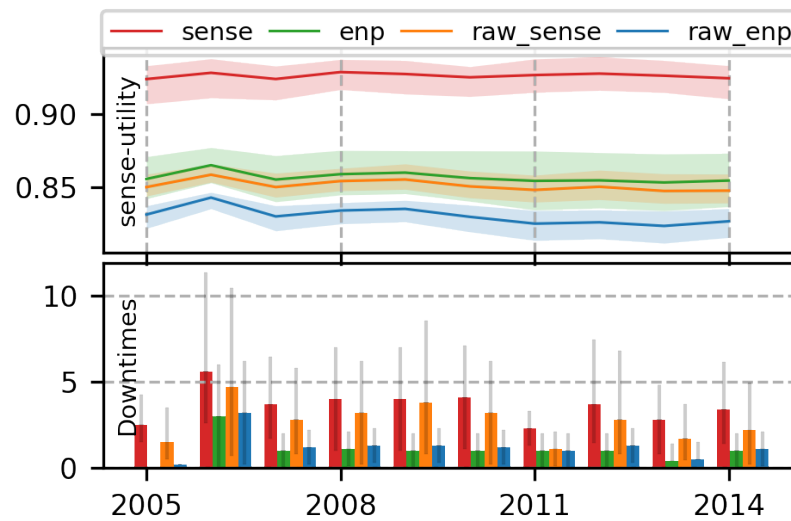


Figure 14. *sense* and *enp* learn using safe action definitions which result in robust and intelligent policies. Consequently during the test phase, *sense* and *enp* score much higher utilities at much lower downtimes compared to traditional solutions (*raw_sense* and *raw_enp*).

7.1.4. Effect of Size of NN

We also evaluate agents based on our MDP using a smaller NN. We do this to ensure that our results are superior because of our MDP and not simply because of a larger NN. We evaluate *tiny_sense* and *tiny_enp* with 64 nodes in their hidden layer (≈ 5 k parameters) that are otherwise identical to *sense* and *enp* agents which have 256 nodes (≈ 70 k parameters). We observe from Figures 15 and 16 that the learning and testing behaviour of *tiny_sense* and *tiny_enp* do not differ significantly from that of *sense* and *enp*. This puts aside our suspicion that our solutions are superior just because we use a larger NN with more computation. The results from Figures 15 and 16 indicate that it is possible to learn intelligent policies with small NNs and reduce computation resources required for RL-based solutions on the edge. However, a downside to using smaller NNs is the gradual loss in training stability (notice the large variation in sense-utility for *tiny_sense* during test in Figure 16 (top)). As we reduce the size of NN further, it becomes difficult to converge during learning. One way to compensate for the loss in learning stability would be to use specialized RL algorithms and NN architectures depending on the hardware platform and application scenario.

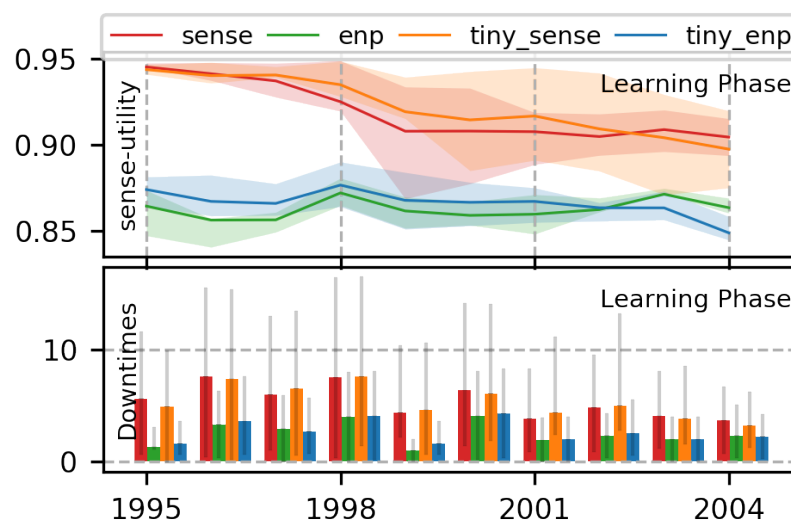


Figure 15. Learning performance of agents with smaller networks.

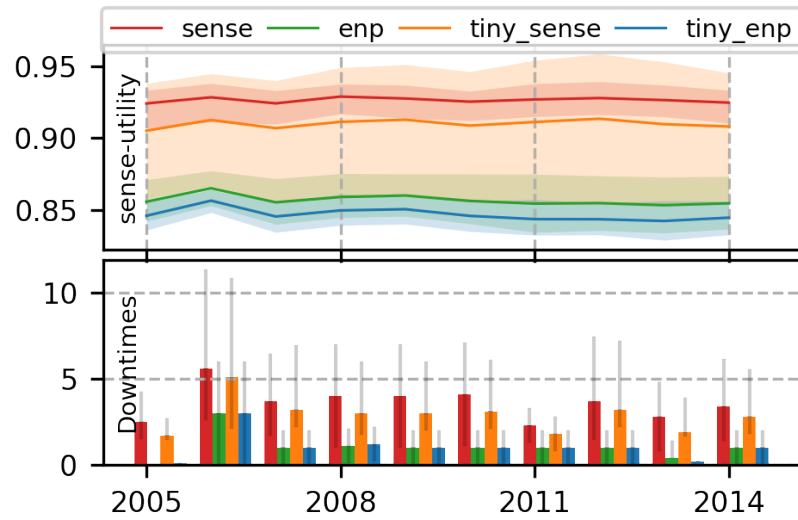


Figure 16. Test performance of agents with smaller networks.

7.2. Runtime Tradeoffs

We now shift our discussion to how it may be possible to optimize runtime tradeoffs between two or more objectives over a space of preferences. We consider the dual-objective case where the single-task EHWSN agent has to optimize between maximizing the sense-utility u_t^{sense} , and the ENP-utility u_t^{ENP} . ω is the user-defined parameterized priority for sense-utility w.r.t. ENP-utility. The ultimate goal of the MORL agent is to maximize the node-utility, $w_t = \omega u_t^{sense} + (1 - \omega) u_t^{ENP}$.

7.2.1. Limitations of Traditional Scalarization Methods

We first demonstrate the limitations of traditional RL methods that attempt to optimize over multiple objectives using scalarization. Figure 17 shows *mul_scalar* (purple) that scalarizes different objective rewards by multiplying them together as in [7,50,52]. Its reward function is $r = u^{sense} \times u^{ENP}$. This agent cannot tradeoff between sense-utility and ENP because its reward function is fixed and does not contain the ω parameter. The resulting policy is an “average” between maximizing sense-utility and ENP-utility and it is not clear how one can tweak the reward function with a single parameter to gradually bias the agent to optimize any one of the objectives.

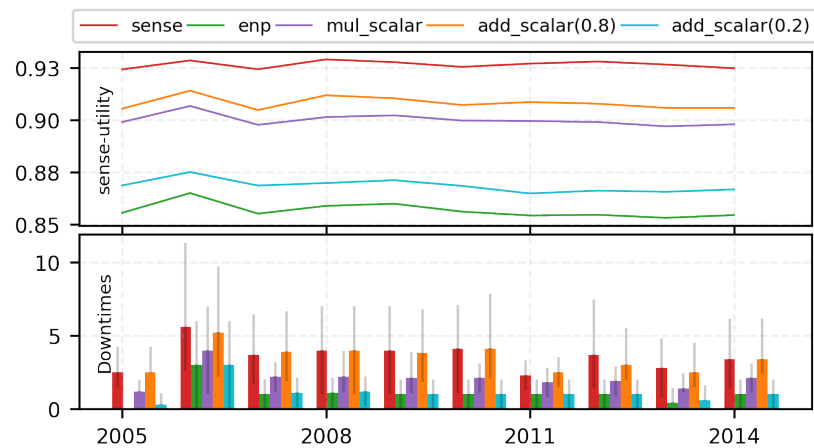


Figure 17. Scalarization methods for MORL: *add_scalar* can tradeoff only if the relative priorities are known before training. It is not clear what objective *mul_scalar* is optimizing.

add_scalar uses the reward values obtained by a linear combination of the different objective rewards weighted by their relative preferences [51,52]. For e.g., *add_scalar*(0.8) in Figure 17 uses a reward function defined by $r = \omega u^{\text{sense}} + (1 - \omega)u^{\text{ENP}}$ where $\omega = 0.8$. The resultant policy sacrifices energy neutrality (i.e., higher downtimes) for higher sense utility. Similarly, *add_scalar*(0.2) trades off sense-utility for lower downtimes (better ENP). By altering the value of ω , the user can trade off between sense-utility and ENP. However, this method requires the user to fix the value of ω before training the RL agent. If the user requires a different ω , the agent needs to be retrained with a new reward function corresponding to the new value of ω . As a result, this method cannot be used to tradeoff during runtime. This is a major disadvantage because the parameter ω can change at every timestep. Thus, we can see that it is not possible for the user to tradeoff at runtime using traditional scalarization methods. We refer the reader to [52] for an in-depth analysis of different reward scalarization schemes for ENO.

7.2.2. Trading Off with Runtime MORL (Algorithm 1)

We use *Runtime MORL* algorithm (Algorithm 1) in order to tradeoff between objectives at runtime by varying the parameter ω . This is implemented as the *morl_runtime*(ω) agent. *morl_runtime*(ω) uses the actor-critic pairs from *sense* and *enp* agents to generate policies that can tradeoff at runtime.

In Figure 18, we compare between *morl_runtime*(ω) and *add_scalar*(ω) to analyze their tradeoff characteristics. We observe that our *morl_runtime*(ω) agent can indeed trade-off by varying ω at runtime without any retraining. High sense-priority ($\omega = 0.8$, green) increases utility and downtimes and vice versa for low priority ($\omega = 0.2$, red). We note that the range of tradeoffs is lesser for *morl_runtime* than *add_scalar*. This is because the tradeoff takes place in the value space for *morl_runtime* and in the reward space for *add_scalar*. Although the range of tradeoffs may be decreased in *morl_runtime*, it is more optimal. This can also be observed in Figure 18 where *morl_runtime*(0.2) (pink) consistently extracts much higher utility than *add_scalar*(0.2) (cyan) for similar energy-neutrality. Likewise, *add_scalar*(0.8) (orange) has disproportionately higher downtimes for only a slight increase in sense-utility than our *morl_runtime*(0.8) (green).

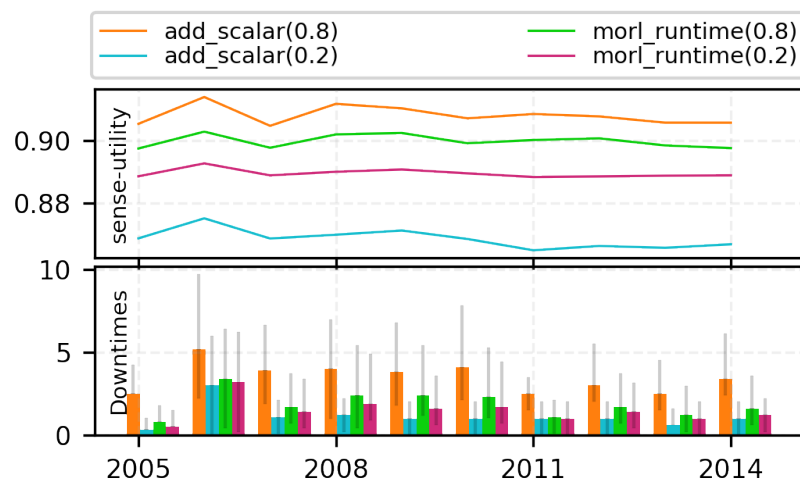


Figure 18. *morl_runtime*(ω) (Algorithm 1) can tradeoff sense-utility with energy neutrality (downtimes) at runtime.

Thus, we see that our proposed *Runtime MORL* algorithm can generate better policies than scalarization methods that can tradeoff w.r.t. ω at runtime.

7.3. Learning Multi-Objective RL Policies for ENO

The previous results demonstrate how we can use Algorithm 1 for runtime tradeoffs using pre-trained greedy agent actor-critic pairs. We now consider a more realistic scenario for EWHNSs where we don't have pre-trained greedy agents. The MORL agent has to learn these actors and critics tabula rasa and use them for runtime tradeoffs between different objectives. We consider the case for single-task EWHNS (two objectives) and dual-task EWHNS (three objectives). These are obviously harder learning problems that require efficient learning within a larger exploration space.

7.3.1. 2-Objective MOO with Off-Policy MORL (Algorithm 2)

We train a single-task EWHNS MORL agent, *morl_offpolicy*, that has to learn policies for runtime tradeoffs between two objectives (maximizing utility and minimizing downtimes). Figure 19 compares the test performance for *morl_offpolicy*(ω) for different values of the preference parameter ω against our baseline SORL agents *sense* and *enp*. *morl_offpolicy* learns the greedy actor-critics for both *sense* and ENO objectives and trades off between them using Algorithm 2. This is a difficult learning problem because *morl_offpolicy* has to learn two different actor-critic pairs, optimized for two different conflicting objectives using the same experience replay stream. Algorithm 2 achieves this by using off-policy corrections [75,76] (see Section 5.3). This is very different from the learning process of SORL agents like *sense* and *enp* where they learn using experience samples only for their respective objectives.

In Figure 19, it is clear that changing ω from 0.1 to 0.8 increases sensing utility with corresponding tradeoffs in energy neutrality. Both *morl_offpolicy*(0.1) and *morl_offpolicy*(0.8) (blue and brown bars) incur slightly higher losses (and higher variations) in energy neutrality compared to the *sense* and *enp* baselines (red and green bars). This is expected because *morl_offpolicy* uses the same amount of training as SORL baselines to learn a harder problem so there is a slight degradation in stability and optimality.

Figure 20 compares the cumulative learning costs between *morl_offpolicy* and traditional scalarization methods (*add_scalar* and *mul_scalar*). We observe that the gross learning cost of *morl_offpolicy* is not much higher than that of other methods. Thus, *morl_offpolicy* can learn a more difficult problem (i.e., multiple actor-critic policies that can tradeoff at runtime) with similar learning costs as previous methods.

We analyze the learning performance of *morl_offpolicy* in more detail in Figure 21 where we compare the learning costs (downtimes) between *morl_offpolicy* and SORL baseline agents. We observe that the learning costs are somewhere in between that of *sense* and *enp*. This is encouraging because this means we do not need exorbitant learning costs for a MORL policy using our framework. The reason for this efficient learning is as follows. During the early stages of training, the actor-critic pairs (like that of *sense*) are imperfect and prone to taking very extreme and potentially dangerous actions to maximize their objectives. For SORL agents with a single actor-critic pair, this results in large downtimes which increases the learning costs. Alternatively, actor-critic pairs which are optimized to minimize negative rewards (like *enp*) are too cautious, resulting in insufficient exploration, lost opportunities for maximization, and therefore converge to non-optimal policies. However, since *morl_offpolicy* has two actor-critic pairs that influence the exploration policy from two opposing directions (maximizing utility and minimizing downtimes), the final policy is a compromise between them that checks the agent from committing extreme actions that seem lucrative in the short term but are dangerous in the long run. Thus, even with imperfect actors and critics, the agent can avoid unsafe/non-optimal state-action spaces. Thus, with our method, the agent explores the state space in a safe manner and learns a harder problem more efficiently than traditional methods.

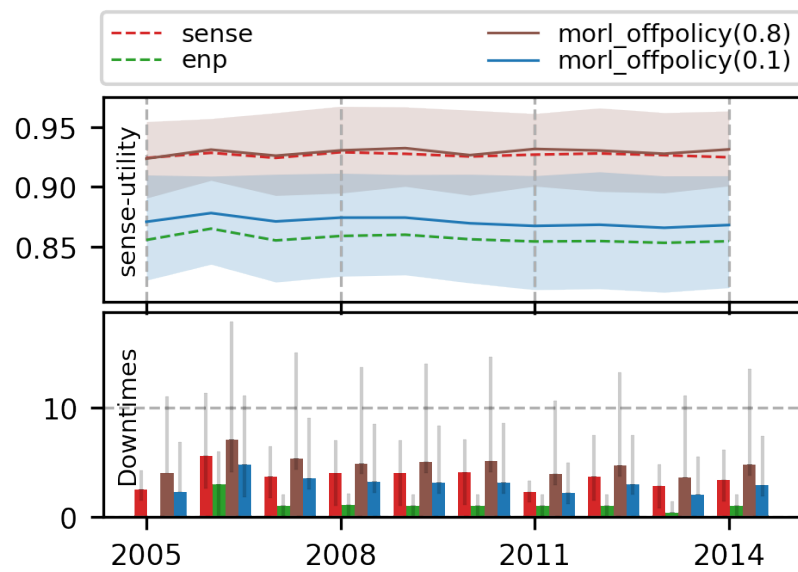


Figure 19. *morl_offpolicy* (ω) learns greedy actor-critics that can tradeoff between sense and ENO objectives using Algorithm 2.

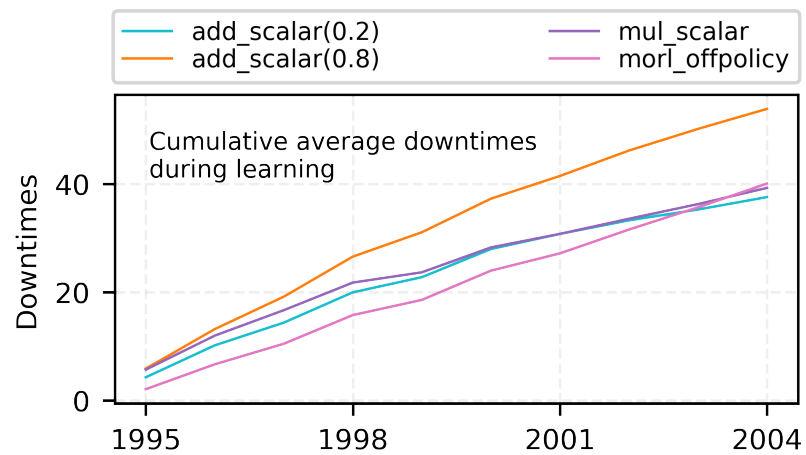


Figure 20. *morl_diff* has learning costs comparable to other scalarization methods in spite of a harder learning problem.

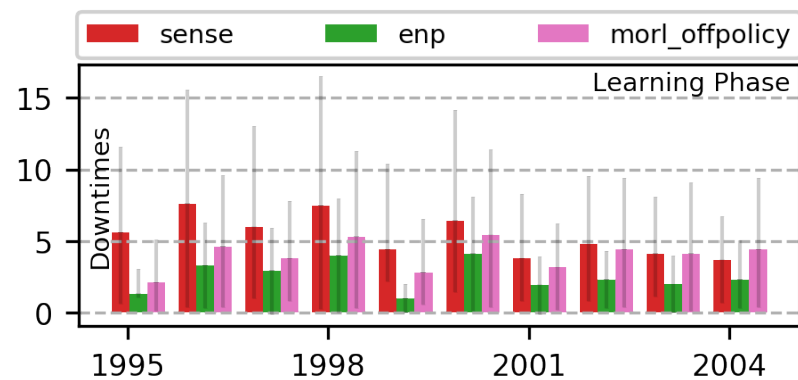


Figure 21. *morl_offpolicy* has lower learning costs compared to *sense* and *enp*. This is because the opposing greedy actor-critics for MORL check each other from committing extreme actions.

7.3.2. 3-Objective MOO with Off-Policy MORL (Algorithm 2)

Finally, we consider the case of the dual-task EHWSN. Here, the MORL agent has to learn policies that tradeoff between *three* objectives (maximizing sense-utility, maximizing transmission-utility, and minimizing downtimes). The tradeoffs are made at each timestep based on the user priority $\omega = (\omega_{sense}, \omega_{tx}, \omega_{ENP})$. We train the *morl_multi* agent using Algorithm 2. We use the same discount factors for all tasks (to simplify analysis). The action space is two-dimensional in this case and so the convex hull is a 2-D polygon from which potentially optimal actions are sampled. During testing, we compare the performance of *morl_multi* for different values of constant ω . We observe whether the results policies can maximize the different objectives and tradeoff w.r.t. ω .

In Figure 22, we first observe how *morl_multi* trades off its energy neutrality with changing ω . When energy neutrality has low priority ($\omega_{ENP} = 0.1$, blue and orange), the downtimes (bottom bar plot) are much higher than when $\omega_{ENP} = 0.7$ (green and red). As a result of this trade off, the corresponding utilities for $\omega_{ENP} = 0.1$ are much higher than that of $\omega_{ENP} = 0.7$ (top and middle figures).

Secondly, we observe how the agent trades off between *sense-utility* and *tx-utility*. Let us consider two cases where the ENO objective has the same preference i.e., $\omega_{ENP} = 0.1$ (blue and orange). The blue line corresponds to a higher preference for sensing than for transmission (i.e., $\omega_{sense} > \omega_{tx}$) and vice versa for the orange line. Thus, the blue line scores higher in sense-utility than the orange line (top figure). However, it scores lower in tx-utility compared to the orange line (middle figure). A similar observation can be made when $\omega_{ENP} = 0.7$ (green and red lines). This clearly demonstrates that *morl_multi* can trade-off between its different objectives.

Thirdly, we analyze the tradeoff between sensing-utility and ENP. In the top figure of Figure 22, we observe that as we progressively decrease the priority for sensing and increase the priority for energy neutrality, the agent decreases its sense-utility and downtimes correspondingly (blue \rightarrow orange \rightarrow green \rightarrow red) i.e., it becomes more energy-neutral at the expense of lower utility. A similar trend can be observed in the middle figure for tx-utility (orange \rightarrow blue \rightarrow red \rightarrow green). However due to the concavity of the *tx-utility*, there is a larger drop when the tx-priority ω_{tx} is reduced from 0.7 to 0.2. The tradeoff between sensing-utility and ENP is very clear when we observe the blue and red lines/bars. Both the blue and red lines correspond to $\omega_{tx} = 0.2$ and so their tx-utility is very similar (middle figure). However, the blue line corresponding to $\omega_{sense} > \omega_{ENP}$ has a much higher sense-utility (see top figure) than the red line ($\omega_{sense} < \omega_{ENP}$) at the expense of higher downtimes (see bottom figure).

Finally, we discuss the learning costs for *morl_multi* shown in Figure 23. We observe that it has an acceptable number of average downtimes (less than 15) during testing and learning, which is competitive with previous methods [8]. This means that *morl_multi* policies are stable, convergent, and energy neutral in spite of having to learn three different greedy actor-critics within the same training period as previous methods. This is primarily due to off-policy corrections in Algorithm 2 and safe exploration induced by safe actions as well as auto-regulation among the greedy agents. Thus, our framework can learn to optimize between three objectives successfully in dual-task EHWSNs, without a drastic increase in learning costs, which indicates that it can be scaled to any number of tasks as required. With additional tasks, their convex hull formed by greedy actions will have correspondingly more dimensions. This means that we will have to sample and evaluate more actions from this hull which increases the computational requirements. One can compensate for this through a more coarse-grained sampling of actions at the expense of fewer optimal solutions.

From the above observations and analysis, we show that our proposed MORL framework for ENO of EHWSNs is not only feasible but also superior to previous methods. We can learn more optimal policies with lower learning costs and tradeoffs at runtime. This can be attributed to our more appropriate MDP formulation of the ENO problem. Also, by compromising between compute-intensive MORL methods and elitist MC/EA methods, our proposed MORL algorithms are a feasible solution for resource-constrained EHWSN.

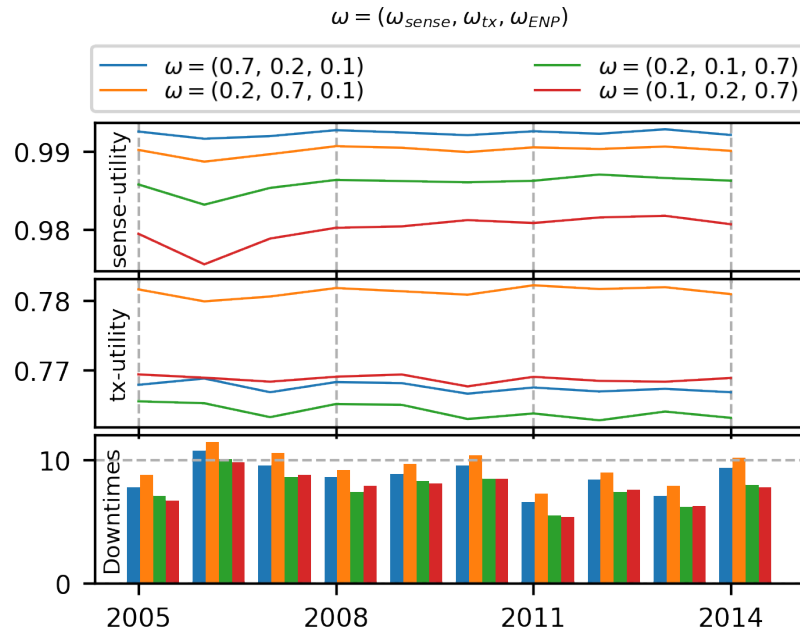


Figure 22. *morl_multi* agent has lower downtimes when ENO has higher priority (green and red) than when it is lower (blue and orange). Given the same ω_{ENP} , the agent trades off between sense-utility and tx-utility using the values of ω_{sense} and ω_{tx} .

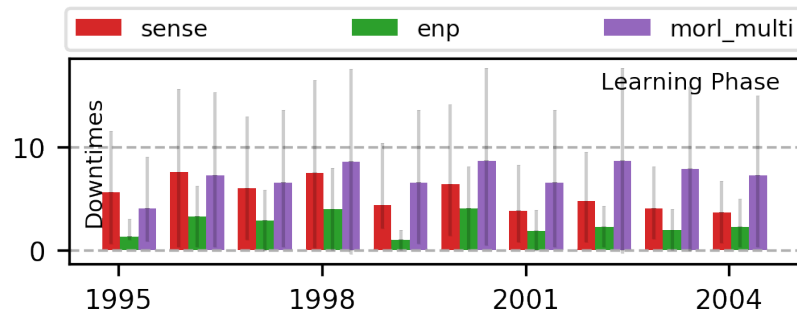


Figure 23. *morl_multi* has acceptable learning costs (slightly higher than *sense*) even though the learning problem is much harder.

8. Conclusions and Future Directions

IoT embedded systems require MOO to coordinate and optimize its limited resource among multiple tasks. Traditional heuristics (like MC roll-outs, EA) are unsuited for this because they assume time-invariant objective functions whereas node-level MOO generally requires time-varying objective functions. Other alternative methods either result in non-optimal solutions or have very high computation costs making them unsuitable for embedded systems.

We provide a MORL framework for MOO in IoT embedded devices in order to overcome this problem. The framework is made up of general MOMDP and two low-compute MORL algorithms. These algorithms offer a workable solution for resource-constrained EHWSNs by falling somewhere between non-adaptive heuristics and compute-intensive MORL approaches. With our proposed framework, embedded devices can learn to make tradeoffs while maintaining reasonable learning costs. We use single-task and dual-task EHWSNs as an example application and demonstrate MOO for ENO. We create an appropriate MOMDP for the EHWSN system model and assess the performance of our suggested algorithms. Our findings demonstrate that adopting our framework allows

for the run-time tradeoff of objectives and the learning of near-optimal policies at lower learning costs.

Our MORL solution still needs to be improved to be implemented in IoT systems with severe resource constraints. Since our framework can theoretically be applied to other less compute-intensive RL algorithms, some alternatives to DDPG include using tabular approaches [7,9], linear function approximation [6,11,50], or distributed learning [8]. In our other paper [8], we show that inefficient exploration is one of the major causes of such instability and propose a distributed RL method with novel ϵ -greedy exploration strategies to not only minimize the learning time and computational costs. This is orthogonal to this work and can be combined together to get more powerful policies at lower learning costs.

Another strategy to implement MORL NN models in IoT embedded devices would be to compress the NN model. Recent works have shown that it is possible to compress a large 16 GB ImageNet model and fit it into a micro-controller [77] without compromising too much on accuracy and latency. Encouraging results have been reported in [78] where the authors implement Deep RL to optimize the modulation scheme for software-defined radio in real-time low-power hardware.

Author Contributions: Conceptualization, S.S.; methodology, S.S.; software, S.S.; validation, S.S., M.K., and H.N.; formal analysis, S.S.; investigation, S.S.; resources, S.S., M.K. and H.N.; data curation, S.S.; writing—original draft preparation, S.S.; writing—review and editing, S.S., M.K., and H.N.; visualization, S.S.; supervision, M.K. and H.N.; project administration, M.K. and H.N.; funding acquisition, S.S., M.K., and H.N. All authors have read and agreed to the published version of the manuscript.

Funding: This work was partially supported by JST CREST Grant Number JPMJCR20F2 and JSPS KAKENHI Grant Number 18J20946.

Institutional Review Board Statement: Not applicable.

Informed Consent Statement: Not applicable.

Data Availability Statement: Not applicable.

Acknowledgments: The authors would like to thank Yuan He for his valuable input and comments.

Conflicts of Interest: The authors declare no conflict of interest.

Abbreviations

The following abbreviations are used in this manuscript:

EHWSN	Energy Harvesting Wireless Sensor Nodes
IoT	Internet of Things
SoC	System-on-Chips
ENO	Energy Neutral Operation
ENP	Energy Neutral Performance
MDP	Markov Decision Process
RL	Reinforcement Learning
DL	Deep Learning
DRL	Deep Reinforcement Learning
MORL	Multi-Objective Reinforcement Learning
SORL	Single-Objective Reinforcement Learning
MOO	Multi-Objective Optimization
GA	Genetic Algorithms
JMA	Japan Meteorological Agency
WSN	Wireless Sensor Network
MC	Monte-Carlo
EA	Evolutionary Algorithms
PSO	Particle Swarm Optimization
QoS	Quality of Service

References

1. Ma, D.; Lan, G.; Hassan, M.; Hu, W.; Das, S.K. Sensing, Computing, and Communications for Energy Harvesting IoTs: A Survey. *IEEE Commun. Surv. Tutor.* **2019**, *22*, 1222–1250. [\[CrossRef\]](#)
2. Nakamura, Y.; Arakawa, Y.; Kanehira, T.; Fujiwara, M.; Yasumoto, K. Senstick: Comprehensive sensing platform with an ultra tiny all-in-one sensor board for iot research. *J. Sens.* **2017**, *2017*, 6308302. [\[CrossRef\]](#)
3. Vamplew, P.; Yearwood, J.; Dazeley, R.; Berry, A. On the limitations of scalarisation for multi-objective reinforcement learning of pareto fronts. In Proceedings of the Australasian Joint Conference on Artificial Intelligence, Auckland, New Zealand, 1–5 December 2008; Springer: Berlin/Heidelberg, Germany, 2008; pp. 372–378.
4. Sutton, R.S.; Barto, A.G. *Reinforcement Learning: An Introduction*; MIT Press: Cambridge, MA, USA, 2018.
5. Blasco, P.; Gunduz, D.; Dohler, M. A learning theoretic approach to energy harvesting communication system optimization. *IEEE Trans. Wirel. Commun.* **2013**, *12*, 1872–1882. [\[CrossRef\]](#)
6. Ortiz, A.; Al-Shatri, H.; Li, X.; Weber, T.; Klein, A. Reinforcement learning for energy harvesting point-to-point communications. In Proceedings of the 2016 IEEE International Conference on Communications (ICC), Kuala Lumpur, Malaysia, 22–27 May 2016; pp. 1–6.
7. Hsu, R.C.; Liu, C.T.; Wang, H.L. A reinforcement learning-based ToD provisioning dynamic power management for sustainable operation of energy harvesting wireless sensor node. *IEEE Trans. Emerg. Top. Comput.* **2014**, *2*, 181–191. [\[CrossRef\]](#)
8. Shresthamali, S.; Kondo, M.; Nakamura, H. Power Management of Wireless Sensor Nodes with Coordinated Distributed Reinforcement Learning. In Proceedings of the 2019 IEEE 37th International Conference on Computer Design (ICCD), Abu Dhabi, United Arab Emirates, 17–20 November 2019; pp. 638–647.
9. Shresthamali, S.; Kondo, M.; Nakamura, H. Adaptive power management in solar energy harvesting sensor node using reinforcement learning. *ACM Trans. Embed. Comput. Syst. (TECS)* **2017**, *16*, 181. [\[CrossRef\]](#)
10. Fraternali, F.; Balaji, B.; Agarwal, Y.; Gupta, R.K. ACES—Automatic Configuration of Energy Harvesting Sensors with Reinforcement Learning. *arXiv* **2019**, arXiv:1909.01968.
11. Sawaguchi, S.; Christmann, J.F.; Lesecq, S. Highly adaptive linear actor-critic for lightweight energy-harvesting IoT applications. *J. Low Power Electron. Appl.* **2021**, *11*, 17. [\[CrossRef\]](#)
12. Parisi, S.; Pirota, M.; Smacchia, N.; Bascetta, L.; Restelli, M. Policy gradient approaches for multi-objective sequential decision making. In Proceedings of the 2014 International Joint Conference on Neural Networks (IJCNN), Beijing, China, 6–11 July 2014; pp. 2323–2330.
13. Pirota, M.; Parisi, S.; Restelli, M. Multi-objective reinforcement learning with continuous pareto frontier approximation. In Proceedings of the Twenty-Ninth AAAI Conference on Artificial Intelligence, Austin, TX, USA, 25–30 January 2015.
14. Yang, R.; Sun, X.; Narasimhan, K. A generalized algorithm for multi-objective reinforcement learning and policy adaptation. In Proceedings of the Advances in Neural Information Processing Systems, Vancouver, BC, Canada, 8–14 December 2019; pp. 14636–14647.
15. Mnih, V.; Kavukcuoglu, K.; Silver, D.; Rusu, A.A.; Veness, J.; Bellemare, M.G.; Graves, A.; Riedmiller, M.; Fidjeland, A.K.; Ostrovski, G.; et al. Human-level control through deep reinforcement learning. *Nature* **2015**, *518*, 529. [\[CrossRef\]](#)
16. Silver, D.; Huang, A.; Maddison, C.J.; Guez, A.; Sifre, L.; Van Den Driessche, G.; Schrittwieser, J.; Antonoglou, I.; Panneershelvam, V.; Lanctot, M.; et al. Mastering the game of Go with deep neural networks and tree search. *Nature* **2016**, *529*, 484. [\[CrossRef\]](#)
17. Sudevalayam, S.; Kulkarni, P. Energy harvesting sensor nodes: Survey and implications. *IEEE Commun. Surv. Tutor.* **2011**, *13*, 443–461. [\[CrossRef\]](#)
18. Kansal, A.; Hsu, J.; Zahedi, S.; Srivastava, M.B. Power management in energy harvesting sensor networks. *ACM Trans. Embed. Comput. Syst.* **2007**, *6*, 32. [\[CrossRef\]](#)
19. Shresthamali, S.; Kondo, M.; Nakamura, H. Multi-objective Reinforcement Learning for Energy Harvesting Wireless Sensor Nodes. In Proceedings of the 2021 IEEE 14th International Symposium on Embedded Multicore/Many-core Systems-on-Chip (MCSoc), Singapore, 20–23 December 2021; pp. 98–105.
20. Vigorito, C.M.; Ganesan, D.; Barto, A.G. Adaptive control of duty cycling in energy-harvesting wireless sensor networks. In Proceedings of the 2007 4th Annual IEEE Communications Society Conference on Sensor, Mesh and Ad Hoc Communications and Networks, San Francisco, CA, USA, 18–21 June 2007; pp. 21–30.
21. Sharma, V.; Mukherji, U.; Joseph, V.; Gupta, S. Optimal energy management policies for energy harvesting sensor nodes. *IEEE Trans. Wirel. Commun.* **2010**, *9*, 1326–1336. [\[CrossRef\]](#)
22. Ozel, O.; Tutuncuoglu, K.; Yang, J.; Ulukus, S.; Yener, A. Transmission with energy harvesting nodes in fading wireless channels: Optimal policies. *IEEE J. Sel. Areas Commun.* **2011**, *29*, 1732–1743. [\[CrossRef\]](#)
23. Peng, S.; Low, C. Prediction free energy neutral power management for energy harvesting wireless sensor nodes. *Ad Hoc Netw.* **2014**, *13*, 351–367. [\[CrossRef\]](#)
24. Cionca, V.; McGibney, A.; Rea, S. MALLIEC: Fast and Optimal Scheduling of Energy Consumption for Energy Harvesting Devices. *IEEE Internet Things J.* **2018**, *5*, 5132–5140. [\[CrossRef\]](#)
25. Jia, R.; Zhang, J.; Liu, X.Y.; Liu, P.; Fu, L.; Wang, X. Optimal Rate Control for Energy-Harvesting Systems with Random Data and Energy Arrivals. *ACM Trans. Sens. Netw.* **2019**, *15*, 13. [\[CrossRef\]](#)
26. Fu, A.; Modiano, E.; Tsitsiklis, J.N. Optimal transmission scheduling over a fading channel with energy and deadline constraints. *IEEE Trans. Wirel. Commun.* **2006**, *5*, 630–641. [\[CrossRef\]](#)

27. Lei, L.; Kuang, Y.; Shen, X.S.; Yang, K.; Qiao, J.; Zhong, Z. Optimal reliability in energy harvesting industrial wireless sensor networks. *IEEE Trans. Wirel. Commun.* **2016**, *15*, 5399–5413. [[CrossRef](#)]
28. Buchli, B.; Sutton, F.; Beutel, J.; Thiele, L. Dynamic power management for long-term energy neutral operation of solar energy harvesting systems. In Proceedings of the 12th ACM Conference on Embedded Network Sensor Systems, Memphis, TN, USA, 3–6 November 2014; pp. 31–45.
29. Geissdoerfer, K.; Jurdak, R.; Kusy, B.; Zimmerling, M. Getting more out of energy-harvesting systems: Energy management under time-varying utility with PreAct. In Proceedings of the 18th International Conference on Information Processing in Sensor Networks, Montreal, QC, Canada, 16–18 April 2019; pp. 109–120.
30. Mao, S.; Cheung, M.H.; Wong, V.W. Joint energy allocation for sensing and transmission in rechargeable wireless sensor networks. *IEEE Trans. Veh. Technol.* **2014**, *63*, 2862–2875. [[CrossRef](#)]
31. GhasemAghaei, R.; Rahman, M.A.; Gueaieb, W.; El Saddik, A. Ant colony-based reinforcement learning algorithm for routing in wireless sensor networks. In Proceedings of the Instrumentation and Measurement Technology Conference Proceedings, IMTC 2007, Warsaw, Poland, 1–3 May 2007; pp. 1–6.
32. Blasco, P.; Gündüz, D. Multi-access communications with energy harvesting: A multi-armed bandit model and the optimality of the myopic policy. *IEEE J. Sel. Areas Commun.* **2015**, *33*, 585–597. [[CrossRef](#)]
33. Chan, W.H.R.; Zhang, P.; Nevat, I.; Nagarajan, S.G.; Valera, A.C.; Tan, H.X.; Gautam, N. Adaptive duty cycling in sensor networks with energy harvesting using continuous-time Markov chain and fluid models. *IEEE J. Sel. Areas Commun.* **2015**, *33*, 2687–2700. [[CrossRef](#)]
34. Xiao, Y.; Han, Z.; Niyato, D.; Yuen, C. Bayesian reinforcement learning for energy harvesting communication systems with uncertainty. In Proceedings of the Communications (ICC), 2015 IEEE International Conference on, London, UK, 8–12 June 2015; pp. 5398–5403.
35. Mihaylov, M.; Tuyls, K.; Nowé, A. Decentralized learning in wireless sensor networks. In Proceedings of the International Workshop on Adaptive and Learning Agents, Budapest, Hungary, 12 May 2009; Springer: Berlin/Heidelberg, Germany, 2009; pp. 60–73.
36. Hsu, J.; Zahedi, S.; Kansal, A.; Srivastava, M.; Raghunathan, V. Adaptive duty cycling for energy harvesting systems. In Proceedings of the 2006 ISLPED, Bavaria, Germany, 4–6 October 2006; pp. 180–185.
37. OpenAI. Faulty Reward Functions in the Wild. 2020. Available online: <https://openai.com/blog/faulty-reward-functions/> (accessed on 4 July 2020).
38. DeepMind. Designing Agent Incentives to Avoid Reward Tampering. 2020. Available online: <https://deepmindsafetyresearch.medium.com/designing-agent-incentives-to-avoid-reward-tampering-4380c1bb6cd> (accessed on 4 July 2020).
39. Everitt, T.; Hutter, M. Reward Tampering Problems and Solutions in Reinforcement Learning: A Causal Influence Diagram Perspective. *arXiv* **2019**, arXiv:1908.04734.
40. Xu, Y.; Lee, H.G.; Tan, Y.; Wu, Y.; Chen, X.; Liang, L.; Qiao, L.; Liu, D. Tumbler: Energy Efficient Task Scheduling for Dual-Channel Solar-Powered Sensor Nodes. In Proceedings of the 56th Annual Design Automation Conference 2019 (DAC'19), Las Vegas, NV, USA, 2–6 June 2019; ACM: New York, NY, USA, 2019; pp. 172:1–172:6. [[CrossRef](#)]
41. Gai, K.; Qiu, M. Optimal resource allocation using reinforcement learning for IoT content-centric services. *Appl. Soft Comput.* **2018**, *70*, 12–21. [[CrossRef](#)]
42. Xu, Y.; Lee, H.G.; Chen, X.; Peng, B.; Liu, D.; Liang, L. Puppet: Energy Efficient Task Mapping For Storage-Less and Converter-Less Solar-Powered Non-Volatile Sensor Nodes. In Proceedings of the 2018 IEEE 36th International Conference on Computer Design (ICCD), Orlando, FL, USA, 7–10 October 2018; pp. 226–233.
43. Dias, G.M.; Nurchis, M.; Bellalta, B. Adapting sampling interval of sensor networks using on-line reinforcement learning. In Proceedings of the 2016 IEEE 3rd World Forum on Internet of Things (WF-IoT), Reston, VA, USA, 12–14 December 2016; pp. 460–465.
44. Murad, A.; Kraemer, F.A.; Bach, K.; Taylor, G. Autonomous Management of Energy-Harvesting IoT Nodes Using Deep Reinforcement Learning. *arXiv* **2019**, arXiv:1905.04181.
45. Ortiz Jimenez, A.P. Optimization and Learning Approaches for Energy Harvesting Wireless Communication Systems. Ph.D. Thesis, Technische Universität Darmstadt, Germany, 2019.
46. Qiu, C.; Hu, Y.; Chen, Y.; Zeng, B. Deep deterministic policy gradient (DDPG)-based energy harvesting wireless communications. *IEEE Internet Things J.* **2019**, *6*, 8577–8588. [[CrossRef](#)]
47. Kim, H.; Shin, W.; Yang, H.; Lee, N.; Lee, J. Rate Maximization with Reinforcement Learning for Time-Varying Energy Harvesting Broadcast Channels. In Proceedings of the 2019 IEEE Global Communications Conference (GLOBECOM), Big Island, HI, USA, 9–13 December 2019; pp. 1–6.
48. Van Huynh, N.; Hoang, D.T.; Nguyen, D.N.; Dutkiewicz, E.; Niyato, D.; Wang, P. Optimal and Low-Complexity Dynamic Spectrum Access for RF-Powered Ambient Backscatter System with Online Reinforcement Learning. *IEEE Trans. Commun.* **2019**, *67*, 5736–5752. [[CrossRef](#)]
49. Long, J.; Büyükoztürk, O. Collaborative duty cycling strategies in energy harvesting sensor networks. *Comput. Aided Civ. Infrastruct. Eng.* **2020**, *35*, 534–548. [[CrossRef](#)]
50. Aoudia, F.A.; Gautier, M.; Berder, O. RLMan: An energy manager based on reinforcement learning for energy harvesting wireless sensor networks. *IEEE Trans. Green Commun. Netw.* **2018**, *2*, 408–417. [[CrossRef](#)]

51. Ferreira, P.V.R.; Paffenroth, R.; Wyglinski, A.M.; Hackett, T.M.; Bilén, S.G.; Reinhart, R.C.; Mortensen, D.J. Multiobjective reinforcement learning for cognitive satellite communications using deep neural network ensembles. *IEEE J. Sel. Areas Commun.* **2018**, *36*, 1030–1041. [\[CrossRef\]](#)
52. Rioual, Y.; Le Moullec, Y.; Laurent, J.; Khan, M.I.; Diguët, J.P. Reward Function Evaluation in a Reinforcement Learning Approach for Energy Management. In Proceedings of the 2018 16th Biennial Baltic Electronics Conference (BEC), Tallinn, Estonia, 8–10 October 2018; pp. 1–4.
53. Liu, C.; Xu, X.; Hu, D. Multiobjective reinforcement learning: A comprehensive overview. *IEEE Trans. Syst. Man, Cybern. Syst.* **2014**, *45*, 385–398.
54. Zeng, F.; Zong, Q.; Sun, Z.; Dou, L. Self-adaptive multi-objective optimization method design based on agent reinforcement learning for elevator group control systems. In Proceedings of the 2010 8th World Congress on Intelligent Control and Automation, Jinan, China, 6–9 July 2010; pp. 2577–2582.
55. Ngai, D.C.K.; Yung, N.H.C. A multiple-goal reinforcement learning method for complex vehicle overtaking maneuvers. *IEEE Trans. Intell. Transp. Syst.* **2011**, *12*, 509–522. [\[CrossRef\]](#)
56. Moffaert, K.V.; Nowé, A. Multi-Objective Reinforcement Learning using Sets of Pareto Dominating Policies. *J. Mach. Learn. Res.* **2014**, *15*, 3663–3692.
57. Shelton, C.R. Importance Sampling for Reinforcement Learning with Multiple Objectives. Ph.D. Thesis, MIT, Cambridge, MA, USA, 2001.
58. Li, K.; Zhang, T.; Wang, R. Deep reinforcement learning for multiobjective optimization. *IEEE Trans. Cybern.* **2020**, *51*, 3103–3114. [\[CrossRef\]](#) [\[PubMed\]](#)
59. Lillicrap, T.P.; Hunt, J.J.; Pritzel, A.; Heess, N.; Erez, T.; Tassa, Y.; Silver, D.; Wierstra, D. Continuous control with deep reinforcement learning. *arXiv* **2015**, arXiv:1509.02971.
60. Yang, Z.; Merrick, K.E.; Abbass, H.A.; Jin, L. Multi-Task Deep Reinforcement Learning for Continuous Action Control. In Proceedings of the IJCAI, Melbourne, Australia, 19–25 August 2017; pp. 3301–3307.
61. Li, C.; Czarnecki, K. Urban Driving with Multi-Objective Deep Reinforcement Learning. *arXiv* **2019**, arXiv:1811.08586.
62. Sharma, M.K.; Zappone, A.; Assaad, M.; Debbah, M.; Vassilaras, S. Distributed power control for large energy harvesting networks: A multi-agent deep reinforcement learning approach. *IEEE Trans. Cogn. Commun. Netw.* **2019**, *5*, 1140–1154. [\[CrossRef\]](#)
63. Ortiz, A.; Al-Shatri, H.; Weber, T.; Klein, A. Multi-Agent Reinforcement Learning for Energy Harvesting Two-Hop Communications with a Partially Observable State. *arXiv* **2017**, arXiv:1702.06185.
64. Jia, J.; Chen, J.; Chang, G.; Tan, Z. Energy efficient coverage control in wireless sensor networks based on multi-objective genetic algorithm. *Comput. Math. Appl.* **2009**, *57*, 1756–1766. [\[CrossRef\]](#)
65. Le Berre, M.; Hnaïen, F.; Snoussi, H. Multi-objective optimization in wireless sensors networks. In Proceedings of the ICM 2011 Proceeding, Istanbul, Turkey, 13–15 April 2011; pp. 1–4.
66. Marks, M. A survey of multi-objective deployment in wireless sensor networks. *J. Telecommun. Inf. Technol.* **2010**, *3*, 36–41.
67. Fei, Z.; Li, B.; Yang, S.; Xing, C.; Chen, H.; Hanzo, L. A survey of multi-objective optimization in wireless sensor networks: Metrics, algorithms, and open problems. *IEEE Commun. Surv. Tutor.* **2016**, *19*, 550–586. [\[CrossRef\]](#)
68. Iqbal, M.; Naeem, M.; Anpalagan, A.; Ahmed, A.; Azam, M. Wireless sensor network optimization: Multi-objective paradigm. *Sensors* **2015**, *15*, 17572–17620. [\[CrossRef\]](#)
69. Konstantinidis, A.; Yang, K.; Zhang, Q. An evolutionary algorithm to a multi-objective deployment and power assignment problem in wireless sensor networks. In Proceedings of the IEEE GLOBECOM 2008—2008 IEEE Global Telecommunications Conference, New Orleans, LA, USA, 30 November–4 December 2008; pp. 1–6.
70. Ahmed, M.M.; Houssein, E.H.; Hassanien, A.E.; Taha, A.; Hassanien, E. Maximizing lifetime of large-scale wireless sensor networks using multi-objective whale optimization algorithm. *Telecommun. Syst.* **2019**, *72*, 243–259. [\[CrossRef\]](#)
71. Jia, J.; Chen, J.; Chang, G.; Wen, Y.; Song, J. Multi-objective optimization for coverage control in wireless sensor network with adjustable sensing radius. *Comput. Math. Appl.* **2009**, *57*, 1767–1775. [\[CrossRef\]](#)
72. Giardino, M.; Schwyn, D.; Ferri, B.; Ferri, A. Low-Overhead Reinforcement Learning-Based Power Management Using 2QoSM. *J. Low Power Electron. Appl.* **2022**, *12*, 29. [\[CrossRef\]](#)
73. Japan Meteorological Agency. Japan Meteorological Agency. 2019. Available online: <https://www.jma.go.jp/jma/menu/menureport.html> (accessed on 6 July 2019).
74. Libelium. Waspote-The Sensor Platform to Develop IoT Projects. Available online: <https://www.libelium.com/iot-products/waspote/> (accessed on 22 January 2021).
75. Fujimoto, S.; Meger, D.; Precup, D. Off-policy deep reinforcement learning without exploration. In Proceedings of the International Conference on Machine Learning, PMLR, Long Beach, CA, USA, 9–15 June 2019; pp. 2052–2062.
76. Kumar, A.; Fu, J.; Tucker, G.; Levine, S. Stabilizing off-policy q-learning via bootstrapping error reduction. *arXiv* **2019**, arXiv:1906.00949.
77. Lin, J.; Chen, W.M.; Lin, Y.; Cohn, J.; Gan, C.; Han, S. Mccunet: Tiny deep learning on iot devices. *arXiv* **2020**, arXiv:2007.10319.
78. Restuccia, F.; Melodia, T. DeepWiERL: Bringing Deep Reinforcement Learning to the Internet of Self-Adaptive Things. In Proceedings of the IEEE INFOCOM 2020—IEEE Conference on Computer Communications, Toronto, ON, Canada, 6–9 July 2020; pp. 844–853.